Cerebral Cortex, April 2018;28: 1087–1104

doi: 10.1093/cercor/bhx009
Advance Access Publication Date: 3 February 2017
Original Article

ORIGINAL ARTICLE

Regulation of Dendritic Spine Morphology in Hippocampal Neurons by Copine-6

Katja Burk[1,†], Binu Ramachandran[1,†], Saheeb Ahmed[1,2,†], Joaquin I. Hurtado-Zavala[1,†], Ankit Awasthi[1,†], Eva Benito[3], Ruth Faram[4], Hamid Ahmad[1,5], Aarti Swaminathan[1], Jeffrey McIlhinney[4], Andre Fischer[3], Pavel Perestenko[4] and Camin Dean[1]

[1]Trans-synaptic Signaling Group, European Neuroscience Institute, Grisebachstrasse 5, 37077 Göttingen, Germany, [2]Department of Diagnostic and Interventional Radiology, University Medical Center Göttingen, Robert Koch Strasse 40, 37075 Göttingen, Germany, [3]German Center for Neurodegenerative Diseases (DZNE) Göttingen, von Siebold Str. 3A, 37075 Göttingen, Germany, [4]MRC Anatomical Neuropharmacology Unit, University of Oxford, Mansfield Road, Oxford OX1 3TH, UK and [5]Johannes Gutenberg University Mainz, Saarstrasse 21, 55122 Mainz, Germany

Address correspondence to Camin Dean, Trans-synaptic Signaling Group, European Neuroscience Institute, Grisebachstrasse 5, 37077 Göttingen, Germany. Email: c.dean@eni-g.de; Pavel Perestenko, MRC Anatomical Neuropharmacology Unit, University of Oxford, Mansfield Road, Oxford OX13TH, UK. Email: pavel.perestenko@pharm.ox.ac.uk

[†]These authors contributed equally to this work.

Abstract

Dendritic spines compartmentalize information in the brain, and their morphological characteristics are thought to underly synaptic plasticity. Here we identify copine-6 as a novel modulator of dendritic spine morphology. We found that brain-derived neurotrophic factor (BDNF) – a molecule essential for long-term potentiation of synaptic strength – upregulated and recruited copine-6 to dendritic spines in hippocampal neurons. Overexpression of copine-6 increased mushroom spine number and decreased filopodia number, while copine-6 knockdown had the opposite effect and dramatically increased the number of filopodia, which lacked PSD95. Functionally, manipulation of post-synaptic copine-6 levels affected miniature excitatory post-synaptic current (mEPSC) kinetics and evoked synaptic vesicle recycling in contacting boutons, and post-synaptic knockdown of copine-6 reduced hippocampal LTP and increased LTD. Mechanistically, copine-6 promotes BDNF-TrkB signaling and recycling of activated TrkB receptors back to the plasma membrane surface, and is necessary for BDNF-induced increases in mushroom spines in hippocampal neurons. Thus copine-6 regulates BDNF-dependent changes in dendritic spine morphology to promote synaptic plasticity.

Key words: dendritic spines, synapse function, synaptic plasticity

Introduction

In the central nervous system, most glutamatergic presynaptic boutons contact postsynaptic sites located on dendritic spines, small protrusions from neuronal dendrites (Nimchinsky et al. 2002; Sala and Segal 2014). Several morphological categories of protrusions from dendrites have been reported, including filopodia, and thin, stubby, branched and mushroom spines (Harris et al. 1992; Tonnesen et al. 2014). This morphology is closely linked

to synaptic efficacy and long-term potentiation of synaptic strength. Filopodia – thin protrusions characterized by a length at least twice as long as their width – are generally thought to be more transient, and often represent nascent post-synaptic sites, which may develop into spines (Yoshihara et al. 2009). While mushroom spines – consisting of a bulbous spine head contacting a presynaptic bouton and a thin spine neck – are thought to represent mature strong synapses (Nimchinsky et al. 2002; Sala and Segal 2014).

The unique morphological properties of mushroom spines allow synapse-specific compartmentalization of synaptic calcium responses (Muller and Connor 1991), biochemical signaling cascades (Svoboda et al. 1996; Lee et al. 2009; Newpher and Ehlers 2009), and electrical properties (Araya et al. 2006; Harnett et al. 2012). This compartmentalization provides an anatomical substrate for memory storage at the single synapse level, whereby individual synapses can be strengthened or weakened by activity during learning (Bliss and Collingridge, 1993). Indeed, dendritic spines remain dynamic after development and well into adulthood where they undergo morphological changes during synaptic plasticity. Induction of long-term potentiation causes new spines to appear (Engert and Bonhoeffer 1999; Maletic-Savatic et al. 1999) and remodel (Bosch et al. 2014), which recruit AMPA receptors upon adopting a mushroom spine morphology (Matsuzaki et al. 2001; Matsuzaki et al. 2004). Induction of long-term depression, on the other hand, results in spine shrinkage, retraction and elimination (Nagerl et al. 2004; Zhou et al. 2004). Brain-derived neurotrophic factor (BDNF), a molecule essential for long-term potentiation (Korte et al. 1995), can promote dendritic spine formation (Ji et al. 2005; Kaneko et al. 2012), which is closely linked to increases in learning and memory (Xu et al. 2009; Yang et al. 2009). Aberrant dendritic spine morphology is also linked to neuropsychiatric disorders (Penzes et al. 2011), including autism (Tang et al. 2014) and Fragile X syndrome (Comery et al. 1997; Irwin et al. 2000).

Actin polymerization and depolymerization is important for plasticity-induced changes in dendritic spine morphology. The GTPases RhoA, Rac1, and Cdc42 regulate the actin cytoskeleton via actin-binding proteins to promote spine morphogenesis (Nakayama et al. 2000; Hotulainen and Hoogenraad 2010). However, the dramatic re-arrangement of dendritic spine membranes during morphological transitions may require additional as yet unknown membrane-targeted proteins. Here we investigated a novel candidate protein that might serve this function called copine-6. Copines are evolutionarily conserved C2-domain-containing proteins that mediate calcium-dependent binding to membrane phospholipids (Creutz et al. 1998; Tomsig et al. 2003). Copine-6 was identified in a screen of mRNAs upregulated by kainate injection in the brain, and its mRNA is also upregulated by high frequency stimulation in the hippocampus (Nakayama et al. 1998). It may therefore sense changes in intracellular calcium concentration during neuronal plasticity. However, the functional role of copine-6 in the brain is not well understood.

Here, we show that copine-6 regulates dendritic spine morphology in hippocampal neurons. Copine-6 protein is upregulated and recruited to dendritic spines by BDNF, and is necessary for both the maintenance of normal spine morphology and for BDNF-induced stabilization of mushroom spines. Post-synaptic knockdown of copine-6 in the Schaffer collateral pathway of the hippocampus decreases LTP and increases LTD in hippocampal slices. Copine-6 promotes the recycling of TrkB receptors to the plasma membrane surface and increases BDNF-TrkB-dependent signaling in hippocampal neurons. We propose that activity-dependent regulation of copine-6 levels may control the elimination or generation of spines during synaptic plasticity via BDNF-TrkB.

Materials and Methods

All research involving animals was approved by and done in accordance with the Institutional Animal Care and Ethics Committees of Goettingen University (T10.31) and with German animal welfare laws, and in accordance with the Animals Scientific Procedures Act of 1986 (UK).

Antibodies, Chemicals and Expression Constructs

Antibodies used were: alpha-tubulin, syp clone 7.2, syb2 clone 69.1, Rab-GDI, PSD95, syt1 clone 41.1, syt1 clone 604.1, GAD65, bassoon, homer, vGAT and vGluT1, HA (Synaptic Systems), LDH (Santa Cruz), copine-6 (Abcam; used for Western blots), MAP-2 (Millipore, Enzo Life Sciences Inc.), Doc2a, PKC gamma (R&D Systems), alpha-tubulin, acetyl-tubulin, phospho-ERK (Cell Signaling Technologies), extracellular GluA1 (Calbiochem), extracellular GluA2 and GluN1 (Millipore). The copine-6 antibody used for immunocyto- and immunohistochemistry was raised against full-length copine-6, absorbed against copine-2, affinity purified with copine-6, and found not to react with copines-1, 2, 3, and 7. Secondary antibodies used were: Alexa Fluor 405, 488, 546, and 647 goat anti-chick, mouse, guinea pig, and rabbit were from Invitrogen/Life Technologies. HRP-conjugated secondary antibodies were from BioRad. BDNF, TrkB-Fc, and control Fc were purchased from R&D Systems. All other chemicals were purchased from Sigma. The copine-6-GFP, and YFP-tagged copine-1, 2, 3, and 7 expression constructs were previously described (Perestenko et al. 2010). Copine-6 knockdown ShRNA constructs used were from Qiagen (Cpne6 SureSilencing shRNA Plasmid, cat. No. KR48747G, RefSeq Accession No.: NM_001191113), clone ID 5: CCCCTTCATGGAGATCTATAAGA (copine-6 KD1), and clone ID 7: TACATACCTTCCTGGATTATATC (copine-6 KD2), mixed in equal proportions in transfections for knockdown. The copine-6 rescue construct was generated by introducing silent substitutions into the copine-6 KD1 sequence (CCCCTTCATGGAGATCTATAAGA) as follows: CCCGTTTATGG AAATATACAAAA. The KD1 sequence was chosen for rescue experiments because transfection of this construct alone resulted in complete knockdown of copine-6 in validation experiments (Fig. 3A). Rescue experiments were performed by transfecting equal proportions of the copine-6 KD1 knockdown construct and the copine-6 rescue construct consisting of full-length Myc-tagged copine-6 in the pCMV-Myc vector (Clontech) with the introduced silent mutations. The scrambled shRNA construct sequence used was: GGAATCTCATTCGATGCATAC. LifeAct-RFP was kindly provided by Thomas Dresbach (University of Goettingen Medical School, Goettingen, Germany). HA-TrkB was provided by Yves Barde (via Addgene, plasmid # 39978).

Tissue Preparation

Whole brain, brain regions, and organs were dissected from adult 4-month old mice and homogenized with a glass-Teflon homogenizer in 320 mM sucrose, 4 mM HEPES-KOH, pH 7.4 with 10 strokes at 900 rpm in the presence of protease inhibitors (Roche).

Subcellular Fractionation of Adult Rat Brain

Fractionation was performed as previously described (Huttner et al. 1983). Brains were homogenized in 320 mM sucrose, 4 mM HEPES-KOH, pH 7.4 in a glass-teflon homogenizer (10 strokes at 900 rpm). The homogenate (H) was centrifuged for 10 min at 1000 × g to remove cell debris and pellet nuclei (P1). Supernatants (S1) were then centrifuged for 15 min at 10 000 × g to obtain the crude

synaptosomal fraction (P2), and crude brain cytosol (S2). Synaptosomes were osmotically lysed with 9 vol of ice-cold ddH_2O containing protease-inhibitors (Roche) and homogenized in a glass-teflon homogenizer (3 strokes at 2000 rpm). The homogenate was centrifuged for 20 min at 25 000 × *g* at 4°C to pellet synaptosomal membranes (LP1). The SV-containing supernatant (LS1) was further centrifuged for 2 h at 200 000 × *g* to separate synaptic vesicles (LP2) from the synaptic cytosol (LS2).

Synaptosome Trypsin Cleavage Assay

Synaptosomes were prepared and treated with trypsin as described previously (Boyken et al. 2013). Purified synaptosomes were centrifuged for 3 min at 8700 × *g*, 4°C. The pellet was resuspended in 320 mM sucrose, 5 mM HEPES, pH 8. For trypsin cleavage, a 0.1 mg/ml trypsin stock solution was added to give a final protein–protease ratio of 100:1. Synaptosomes were incubated for 10, 20, 30, 60, or 90 min at 30°C with gentle agitation. This mixture was then centrifuged for 3 min at 8700 × *g*, and the resulting pellet resuspended in sucrose buffer containing 400 µM Pefabloc (Roche) to stop trypsin cleavage activity. Samples were then analyzed by SDS-PAGE and immunoblotting.

Ca^{2+}-dependent Membrane Binding

Tests of calcium-dependent membrane binding of copine-6 were carried out as described previously (Nakayama et al. 1999). Briefly, adult 4-month old mouse brains were homogenized with 10 strokes at 900 rpm in a glass-Teflon homogenizer in 20 mM Tris-HCl, pH 7.4, 1 mM PMSF and 10 µg/ml Leupeptin, supplemented with 1 mM $CaCl_2$ or 1 mM EGTA. The homogenate was incubated for 30 min at 4°C and then centrifuged at 40 000 × *g* for 30 min at 4°C to resolve membrane and cytosolic fractions, which were subjected to SDS-PAGE followed by immunoblotting as described previously.

Immuno-isolation of Synaptic Vesicles

Mouse monoclonal antibodies directed against syb2 and syt1 were coupled to Protein G magnetic Dynabeads (Invitrogen) in PBS for 2 h at 4°C. Antibody-coated beads were added to whole brain S1 fractions and incubated overnight at 4°C. Magnetic beads were separated from immuno-depleted supernatant and washed 3 times with PBS. Bound vesicles were eluted in sample buffer and analyzed by SDS-PAGE and immunoblotting as previously described (Ahmed et al. 2013).

Hippocampal Slice Preparation and Culture

Acute hippocampal slices were prepared as described previously (Ramachandran and Frey 2009). Briefly, 8-week old mice were anesthetized with isoflurane and decapitated. The hippocampus was removed and 200 µm thick slices were cut transversely in ice-cold artificial cerebrospinal fluid (ACSF) containing, in mM: 124 NaCl, 4.9 KCl, 1.2 KH_2PO_4, 2 $MgSO_4$, 2 $CaCl_2$, 24.6 $NaHCO_3$, and 10 D-glucose (saturated with 95% O_2 and 5% CO_2, pH 7.4, ~305 mOsm), using a tissue chopper (Stoelting). Hippocampal slice cultures were prepared as described previously (Fuller and Dailey 2007), and were cultured on Millicell inserts (PICMORG50 from Merck Millipore) in filter culture media (FCM) containing 25% Hanks balanced salt solution, 50% MEM, 25% heat-inactivated horse serum, 2 mM glutamine, 0.044% $NaHCO_3$ and 10 U/ml penicillin-streptomycin, in a humidified 5% CO_2, 37 °C incubator. For Western blot analysis of hippocampal slices treated with BDNF, 5 slices were cultured per insert per condition. Following treatment, slices were floated off inserts in PBS, washed briefly in PBS, and homogenized in 320 mM sucrose, 4 mM HEPES-KOH, at pH 7.4. Protein concentration was determined by BCA assay (Calbiochem) and 15 µg of protein was loaded and analyzed by SDS-PAGE and immunoblotting.

Hippocampal Neuron and HEK Cell Culture and Transfection

Primary dissociated hippocampal neurons were prepared as previously described (Banker and Goslin 1988) with minor modifications. Hippocampi were dissected from E18–E19 rat pups. Cells were mechanically dissociated by trypsinization and trituration. For imaging experiments, neurons were plated on 12 mm glass coverslips coated with 0.04% polyethyleneimine (PEI, Sigma) or 0.5 mg/ml poly-D-lysine (PDL, Sigma) at a density of 50 000–80 000 cells/well. Neurons were cultured in Neurobasal medium supplemented with GlutaMAX, B27, and 100 U/ml penicillin/streptomycin (all from Invitrogen) at 37°C in 5% CO_2. For electrophysiology experiments, hippocampal neurons were plated at a density of 40 000 cells per 12 mm coverslip (at a lower density than for imaging experiments, so that individual miniature excitatory post-synaptic currents (mEPSCs) could be resolved) in DMEM supplemented with 10% fetal bovine serum, glutamax, and pen/strep. After 1–2 days, media was exchanged for Neurobasal medium supplemented with B27, glutamax, and pen/strep. AraC of 5 µM was added at DIV 7-8. Neurons were transfected at DIV7 or DIV10 with Lipofectamine 2000 according to the manufacturer's instructions. For each well of a 24-well plate, 0.75–1 µg DNA/50 µl Neurobasal and 1 µl LF2000/50 µl Neurobasal were incubated separately for 5 min, then mixed together and incubated for an additional 20 min. Media was removed from wells, saved and replaced with 400 µl Neurobasal. The DNA/LF2000 mix was added and cells were put back in the incubator for 2 h. Cells were then washed once with Neurobasal, and conditioned media replaced. For cotransfection of copine constructs with LifeAct-RFP, 0.75 µg DNA total in a ratio of 1:3 of LifeAct-RFP:EGFP, copine-6-GFP, or copine-6 knockdown was added per well. For membrane translocation experiments, HEK293T cells growing on 12 mm coverslips were transfected at approximately 40% confluency: Cells were washed once with PBS and fresh DMEM containing 10% FBS was added. 1.87 µl of 2 M $CaCl_2$, 15 µl transfection buffer (274 mM NaCl, 10 mM KCl, 1.4 mM Na_2HPO_4, 15 mM Glucose, 42 mM HEPES, pH 7.06) and 1 µg Copine-GFP per well were then added and transfected cells were imaged 24–48 h later.

Co-immunoprecipitation

For co-immunoprecipitation of HA-TrkB and copine-6-GFP, cotransfected confluent HEK293 cells growing in 10 cm dishes were harvested in 1 ml IP-Lysis buffer (50 mM Tris-HCl pH 7.5, 150 mM NaCl, 2 mM EDTA, 0.5% NP40, Complete protease inhibitor (Roche)). Cell lysates were then incubated with 30 µl of HA-antibody coupled Protein A/G Dynabeads (Invitrogen) for 2 h at 4°C on a rotator. Uncoupled beads were used for binding controls. Supernatant was saved as the unbound fraction and bound proteins from beads were eluted by incubating beads for 10 min at 95°C in 4X SDS sample buffer. Samples were then analyzed by SDS-PAGE and Western blotting.

Immunocytochemistry and Quantitation

Hippocampal cultures at DIV12-14 were fixed in 4% paraformaldehyde for 20 min, washed 3 times with PBS and incubated for

30 min in antibody buffer (2% donkey serum, 0.1% Triton X-100 and 0.05% NaN_3 in 2× PBS). Cells were then incubated with primary antibodies in antibody buffer for 60 min at room temp or overnight at 4°C. Cells were washed 3 times for 10 min each with PBS, then incubated with fluorescently-tagged secondary antibodies in blocking buffer for 2 h at room temp in the dark. After three 10 min washes with PBS, cells were mounted in Fluoromount-G (Sigma) and sealed with nail polish. Images were acquired on an A1 confocal microscope with Zen software (Carl Zeiss) and a 20× air or 60× oil immersion objective, or a Zeiss Axiovert epifluorescence microscope with a 40× oil immersion objective. All acquisition settings were kept constant between samples in each experiment for quantitation of copine-6 expression in BDNF treated samples, and of syt1 uptake and synaptophysin signal on EGFP, copine-6-GFP and copine-6 knockdown expressing neurons. Images were analyzed using MetaMorph (Molecular Devices, Inc.), Openview (kindly provided by Noam Ziv, Technion, Haifa, Israel), or Image J software. For quantitation of copine-6 in BDNF-treated hippocampal neurons, somas of copine-6-expressing neurons were manually selected and average intensity measured using Metamorph. For copine-6 at synapses, synaptophysin-positive puncta were selected using Openview software, and average copine-6 fluorescence within these puncta was quantified and plotted as average intensity or frequency distribution. For quantitation of synaptophysin and syt1 antibody uptake intensity on EGFP, copine-6-GFP, or copine-6 knockdown neurons, GFP levels in all conditions were set such that signal in all dendritic processes was saturated. This allowed us to mask the transfected cells, including a region approximately 3 μm wide on either side of processes – encompassing all presynaptic boutons terminating on the transfected cell – which was identical in all conditions. Transfected neurons were masked manually, synaptophysin-positive puncta were selected in Openview and the intensity of synaptophysin and syt1 signal in each puncta quantified. For number of synapses (synaptophysin-positive puncta) or number of active synapses (syt1-positive puncta), 20–30 μm stretches of secondary dendrites were selected by GFP signal, and puncta along these dendrites were identified by Openview and counted. To quantify branching in neurons transfected with shRNA, neurons were immunostained with a GFP antibody (A11122, Invitrogen) and branching forks for well-defined neurons were counted. For quantitation of dendritic spine morphology in EGFP, copine-6-GFP or copine-6 knockdown expressing neurons, 4 regions of 20 μm in length were selected per transfected neuron, and the number of filopodia (protrusions with tip width less than base width), stubby spines (protrusions with constant width from base to tip), and mushroom spines (protrusions with head width greater than neck/base width) were counted using Imaris and ImageJ software. PSD95 signal and intensity within these spines was quantified using Metamorph software. For quantitation of surface receptor levels in copine-6 overexpressing or knockdown neurons compared with EGFP, average fluorescence intensity/area of antibody signal against extracellular epitopes of GluA1, GluA2, and GluN1 in cell bodies and proximal dendrites was determined using ImageJ.

Immunohistochemistry

Hippocampal slices from adult 4-month old mice were prepared as described above, fixed in 4% paraformaldehyde in PBS for 30 min and washed 3 times for 20 min each with PBS. After washing, slices were incubated in antibody buffer (2% donkey serum, 0.1% Triton X-100 and 0.05% NaN_3 in PBS) for 30 min at room temp. Then, slices were incubated with primary antibodies in antibody buffer overnight at 4°C. Following primary antibody incubation, slices were washed with PBS 3 times for 20 min each and incubated with fluorescently-tagged secondary antibodies for 2 h at room temp. Slices were washed 3 times for 20 min each with PBS and mounted onto microscope slides with Fluoromount-G (Sigma) and sealed with nail polish. Images were collected using 10× air and 40× oil immersion objectives on a Zeiss A1 laser scanning confocal microscope with Zen software (Carl Zeiss). Digital images were processed using Adobe Photoshop software.

For whole mount sagittal brain sections (Fig. 1B), adult Sprague–Dawley rats were deeply anaesthetized in accordance with the Animals Scientific Procedures Act of 1986 (UK) using isoflurane (4% in O_2), euthanized with pentobarbitone (200 mg/kg), and transcardially perfused via the ascending aorta with 100 ml 0.1 M PBS, followed by 300 ml 4% paraformaldehyde/0.05% glutaraldehyde. Brains were immediately removed and postfixed in 4% paraformaldehyde in 0.1 M PB for 24 h before being sectioned into 50 μM slices in the sagittal plane on a Leica VT1000s vibrating microtome. Sections were collected and washed in PBS. The tissue was blocked in PBS + 5% normal donkey serum, before adding copine-6 antiserum at 1:000 for 48 h at 4°C. Sections were then incubated with secondary antibody, swine anti-rabbit-HRP (1:100) in TBS for 24 h at 4°C, and peroxidase enzyme activity was then visualized with DAB and 0.002% H_2O_2 (in dH_2O) with an optimized reaction time of 5 min. For hippocampal sections (Fig. 1F) and brain sections (Supplementary Fig. 1B), 50 μm vibratome sections were made from adult 4-month old mice using a Leica VT-1000 Vibratome.

HA-TrkB Surface Expression and Recycling Assay

Rat hippocampal neurons growing on coverslips were cotransfected at DIV10 with HA-TrkB and EGFP, copine-6-GFP or copine-6 knockdown constructs. On DIV13, neurons were incubated with anti-HA antibody for 15 min, washed twice with prewarmed Neurobasal medium to remove unbound antibody, and then incubated with 100 ng/ml BDNF for 15 min. Neurons were then washed once with prewarmed Neurobasal medium and fixed with 4% PFA. Surface HA-TrkB was labeled with Alexa 647 secondary antibody for 2 h in triton-free antibody buffer. Cells were then permeabilized and internal HA-TrkB labeled with Alexa 546 secondary antibody for 2 h in antibody buffer containing 0.1% Triton X-100. Coverslips were then mounted in Mowiol and images taken using a Zeiss LSM 710 confocal microscope with a 63× objective. The ratio of surface to internal HA-TrkB was determined by calculating the ratio of surface to internal fluorescence in images of transfected cell bodies.

Recycling of internalized HA-TrkB back to the cell surface was assayed as previously described (Choy et al. 2014). DIV13 neurons were incubated with anti-HA antibody for 15 min, washed twice with prewarmed Neurobasal medium, incubated with 100 ng/ml BDNF for 30 min, washed in 0.04% EDTA in PBS lacking Ca^{2+} and Mg^{2+} to strip remaining surface HA antibody, allowed to recover for 40 min during which internalized HA-TrkB recycled back to the cell surface, fixed and immunostained for surface and internal HA-TrkB with Alexa647 and 546 secondary antibodies, respectively. The amount of HA-TrkB recycled back to the surface was quantified by normalizing to surface versus internal HA-TrkB in control conditions in which cells were fixed after 30 min without BDNF or stripping.

Electrophysiology

DIV 13–19 primary hippocampal neuron cultures were continuously perfused with HEPES buffered saline containing, in

mM: 142 NaCl, 2.5 KCl, 10 HEPES, 10 D-Glucose, 2 $CaCl_2$, 1.3 $MgCl_2$ (pH 7.4, 295 mOsm). mEPSCs were recorded at a command potential of -60 mV in 1 µM TTX (Tocris Biosciences, cat. no. 1069) and 50 µM picrotoxin (Tocris Biosciences, cat. no. 1128). Patch pipettes (3–5 MΩ) were filled with an internal solution containing, in mM: 130 K-gluconate, 10 NaCl, one EGTA, 0.133 $CaCl_2$, 2 $MgCl_2$, 10 HEPES, 3.5 Na-ATP, 1 Na-GTP (pH 7.3, 285 mOsm). Whole-cell patch-clamp recordings (with a command potential of –60 mV) were obtained using a HEKA EPC10 USB double patch clamp amplifier coupled to Patchmaster acquisition software (HEKA Electronics Inc.) for 2 cultures and a NPI ELC-03XS amplifier coupled to a custom-written Igor Pro script for data acquisition for 6 cultures. Signals were low-pass filtered with a Bessel filter at 3.3 kHz. Recordings with a series resistance of less than 25 MΩ which did not change by ≥5 MΩ during the course of the recording, were analyzed using Mini Analysis software v6.0.3 (Synaptosoft Inc.) with an amplitude threshold of 3.5× RMS. At least 170 events (usually 300–450) were analyzed for each recording from a single neuron.

AAV Injections

Cpne6 AAV siRNA Pooled virus Serotype 6 (cat. no. iAAV03825706, from Applied Biological Materials) or control EGFP AAV virus, was injected under ketamine (80 mg/kg)/xylazine (10 mg/kg) anesthesia. Mice were fixed in a stereotaxic device (myNeuroLab) and holes drilled bilaterally at the following coordinates from Bregma: AP: –1.75; ML: +/– 1.0. A fine glass capillary filled with viral vector solution was then inserted –1.5 mm into the DV axis and 1 µl injected at a rate of 0.25 µl/min. The capillary was then slowly retracted and the wound sealed with Histoacryl. Mice were allowed to recover on a heat blanket and monitored closely for 1 week after the operation. Recordings were performed at least 2 weeks after injection, when AAV-dependent expression is maximal and reaches a plateau.

Electrophysiological Recordings from Hippocampal Slices

Acute hippocampal slices from virus-injected mice were prepared as previously described (Ramachandran et al. 2015) from 8 to 10 week old B6/J mice. Animals were anesthetized with isoflurane and decapitated. The brain was removed from the skull and hippocampus dissected. Transverse 400 µm thick hippocampal slices were made using a tissue chopper (Stoelting). Slices were collected in ice-cold ACSF (124 mM NaCl, 4.9 mM KCl, 1.2 mM KH2PO4, 2.0 mM $MgSO_4$, 2.0 mM $CaCl_2$, 24.6 mM $NaHCO_3$, 10.0 mM D-glucose; saturated with 95% O_2 and 5% CO_2; pH 7.4 and 305 mOsm) and incubated in an interface chamber at 32 °C with high oxygen tension maintained by bubbling with 95% O_2 and 5% CO_2 (30 l/h) for 3 h before recordings. Monopolar platinum–iridium electrodes (13303, MicroProbes) used for both recording and stimulating were positioned in the CA1 region. The field excitatory postsynaptic potential (fEPSP) slope was recorded with a Model 1700 differential AC amplifier (A-M Systems) and Power 1401 analog-to-digital converter (Cambridge Electronic Design), and monitored on-line with a custom-made software, PWIN (IFN Magdeburg). The test stimulation strength was determined for each input as the current needed to elicit a field EPSP 40% of maximal slope. Baseline recording began at least 3.30 h after slice preparation, using test stimuli consisting of 4 biphasic constant current pulses (0.2 Hz, 0.1 ms/polarity, averaged) per time point, every 2 min for a minimum of 30 min. LTP was induced with a single theta burst stimulation protocol consisting of 10 burst of 4 pulses at 100 Hz with 200 ms intervals). LTD was induced by low frequency stimulation (LFS) consisting of 900 pulses of 1 Hz for 15 min. Test stimuli were delivered 1, 2, 4, 6 and then every 2 min after theta burst or LFS and up to 60 min.

The input–output relationship of the fEPSP slope or fiber volley versus stimulus intensity was measured by giving 0, 20, 40, 60, 80, and 100 µA stimulation at 60 s. intervals to evaluate postsynaptic response versus presynaptic response in the same hippocampal slices.

To measure the paired-pulse ratio, paired pulses eliciting 40% of the maximal fEPSP were delivered through a single stimulating electrode at 50 ms inter pulse intervals. The ratio of the maximum negative slope of the second pulse to the maximum negative slope of the first pulse was computed as the paired-pulse ratio.

Statistical Analysis

For pairwise comparisons of values indicated in graphs two-tailed Student's *t*-tests of type two were used, following confirmation of equal variance by an *f*-test. A Bonferroni correction was applied for multiple comparisons within datasets. For LTP and LTD experiments, a Mann–Whitney *U* test was performed for statistical comparison. All graphs of quantified data depict average values (mean) and error bars indicate standard error of the mean (s.e.m.).

Results

Copine-6 is Expressed in Dendrites of Hippocampal Pyramidal Neurons

To characterize copine-6 expression, we first examined protein levels in different organs and found copine-6 exclusively in brain, among the tissues tested (Fig. 1*A*; specificity analysis in Supplementary Fig. 1A shows that the copine-6 antibody we generated recognizes overexpressed YFP-tagged copine-6, but not copine-1, 2, 3, or 7). Immunocytochemistry of sagittal rat brain sections revealed widely distributed copine-6 immunoreactivity throughout the brain, with a laminar pattern of expression in the cortex, and high immunoreactivity in the hippocampus, olfactory bulb and striatum, in contrast to the cerebellum (Fig. 1*B*, Supplementary Fig. 1A). A developmental time course of copine-6 levels showed that expression in the brain increased postnatally and remained at high levels in adult brain (Fig. 1*C*). Because copine-6 mRNA is upregulated in the hippocampus in response to stimulation (Nakayama et al. 1998), we treated acute hippocampal slices with 90 mM KCl for 30 min to test the activity-dependence of copine-6 protein expression. Copine-6 protein was significantly increased by this stimulation (Fig. 1*D*,*E*, $P = 0.001$). Acetyl-tubulin, which is also upregulated by neuronal activity, including 90 mM KCl (Pandey and Sharma 2011) served as a positive control, and was significantly increased by KCl treatment ($P = 0.010$). Immunostains of hippocampal slices revealed copine-6 expression in cell bodies and dendrites of pyramidal neurons in the CA1, CA3, and dentate gyrus (Fig. 1*F*), consistent with a previous report (Nakayama et al. 1999).

To examine the cellular and subcellular localization of copine-6 in more detail we immunostained DIV14 hippocampal neuron cultures. Interestingly, copine-6 was highly expressed at varying levels specifically in excitatory neurons (Fig. 1*G*), and was prominent in dendrites (Fig. 1*H*). Copine-6 colocalized with vGluT1 at excitatory synapses, and not with vGAT-positive inhibitory synapses, in these cultures (Fig. 1*I*). To determine if

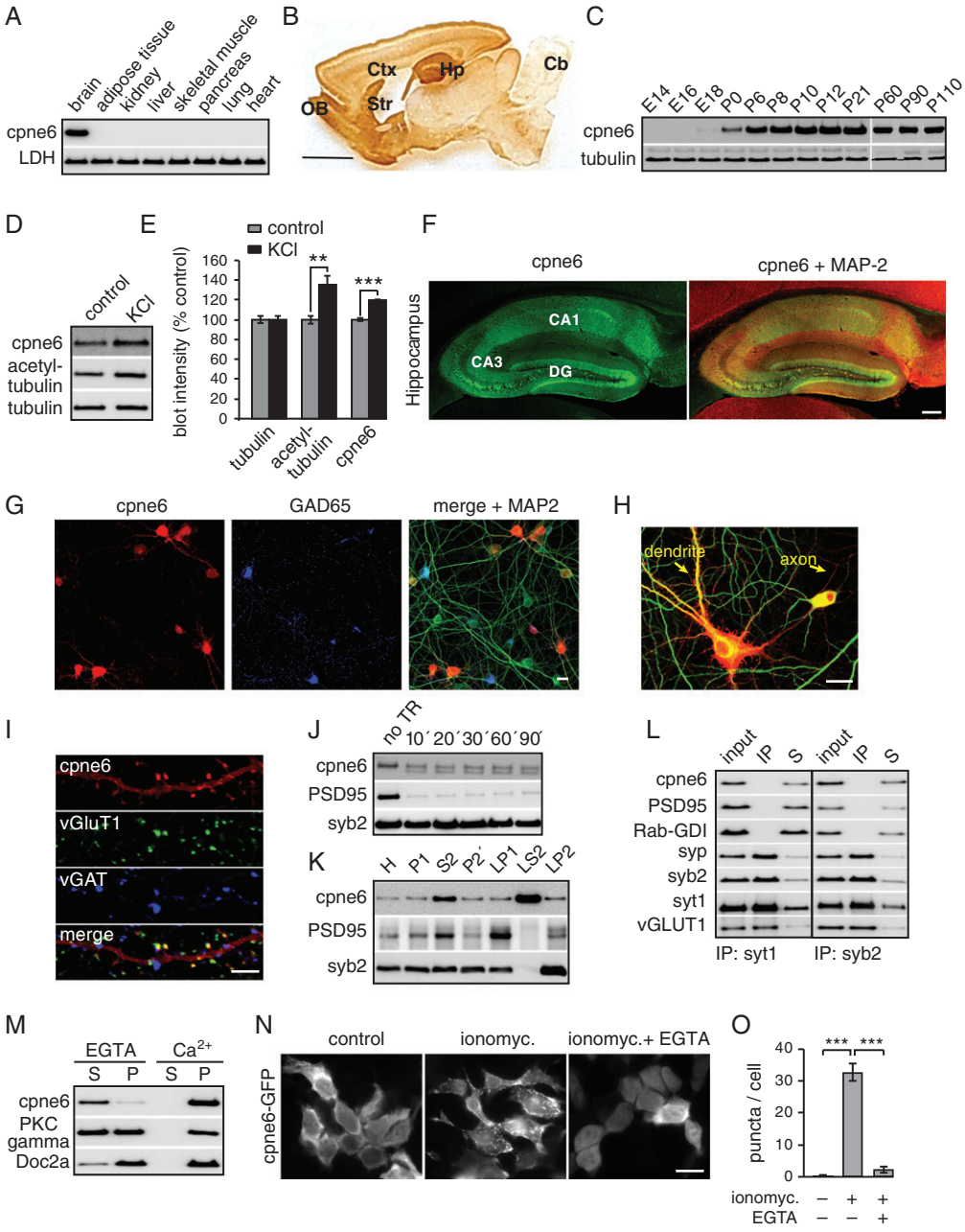

Figure 1. Localization of copine-6. (*A*) Western blot of copine-6 from different organs from adult rats shows expression exclusively in brain. LDH serves as a loading control. (*B*) Copine-6 immunoreactivity in a sagittal section of adult 6 month old rat brain (OB: olfactory bulb, Str: striatum, Ctx: cortex, Hp: hippocampus, Cb: cerebellum; scale bar = 5 mm). (*C*) Developmental expression of copine-6 from whole adult mouse brain at the indicated developmental stages. Tubulin serves as a loading control. (*D*) Western blot of copine-6 in hippocampal slices from 8 week old mice, in control conditions and following stimulation with 90 mM KCl for 30 min. (*E*) Quantitation of Western blot levels in control and treated slices ($n = 3$, statistical significance determined by two-tailed, type two Student's *t*-test, $P \leq 0.01$ = **, $P \leq 0.001$ = ***). Acetyl-tubulin (serving as a positive control) and copine-6 levels are significantly increased by stimulation. (*F*) Immunostain of acute hippocampal slices from 8 week old mice, with copine-6 and MAP2 to mark dendrites. Scale bar = 120 μm. (*G*) Copine-6 does not colocalize with the inhibitory neuron marker GAD65. Scale bar = 10 μm. (*H*) Copine-6 expression in axons and in dendrites marked with MAP2. Scale bar = 10 μm. (*I*) Copine-6 colocalizes with vGluT1 at excitatory synapses, but not with vGAT. Scale bar = 5 μm. (*J*) Trypsinization of synaptosomes from adult mice cleaves post-synaptic proteins including PSD95 and copine-6, but presynaptic proteins (syb2) are protected. (*K*) Western blot of copine-6, PSD95, and syb2 in the indicated subcellular fractions from adult whole brain: homogenate (H), nuclei (P1), crude cytosol (S2), crude synaptosomal fraction (P2'), synaptosomal membranes (LP1), synaptic cytosol (LS2), and crude synaptic vesicles (LP2). (*L*) Copine-6 is not on synaptic vesicles immuno-isolated with syb2 or syt1 antibodies from adult brain. (*M*) Ca^{2+}-dependent association of copine-6 with membranes. In the presence of EGTA, copine-6 remains in the cytosolic supernatant (S), in the presence of Ca^{2+}, copine-6 translocates to membrane pellets (P). (*N*) Localization of copine-6-GFP in transfected HEK cells in control conditions, and in cells treated with 2 μM ionomycin for 30 min to induce calcium influx, or with ionomycin in the presence of 2 mM EGTA. Scale bar = 10 μm. (*O*) Quantitation of localization of copine-6-GFP to membrane patches (puncta) in the indicated conditions ($P \leq 0.001$ = ***).

copine-6 is pre or post-synaptic, we used a trypsin cleavage assay of purified synaptosomes, in which presynaptic proteins are protected from cleavage, while post-synaptic proteins are accessible to trypsin and are cleaved (Boyken et al. 2013). The majority of copine-6 was cleaved by trypsin (Fig. 1*J*), indicating a predominantly post-synaptic location. In comparison, the

presynaptic protein syb2 was fully protected from trypsin cleavage whereas PSD95 was almost entirely cleaved (Fig. 1*J*). In subcellular fractionation experiments, copine-6 was enriched in synaptic cytosol (LS2), and present in synaptosomal membrane fractions (LP1) in lower amounts (Fig. 1*K*). A small portion was found in crude synaptic vesicle fractions (LP2) as well, but copine-6 was not detected on synaptic vesicles immunoisolated with antibodies against syt1 or syb2 (Fig. 1*L*), suggesting that it is likely not associated with synaptic vesicles.

Because copine-6 is reported to bind membranes in the presence of calcium (Nakayama et al. 1999; Perestenko et al. 2010), we separated mouse brain homogenate into cytosol and membrane fractions in the presence of EGTA or calcium to test if copine-6 associates with membranes in a calcium-dependent manner. In the presence of 1 mM EGTA, the majority of copine-6 was detected in the cytosolic fraction. In contrast, in the presence of 1 mM Ca^{2+}, copine-6 was mainly present in the membrane fraction (Fig. 1*M*). The C2 domains of PKC-gamma and Doc2a, which are known to bind phospholipids in a calcium-dependent manner, were used as positive controls (Fig. 1*M*). As a further test we transfected HEK cells with copine-6-GFP. In control conditions, copine-6-GFP was present mainly in the cytosol, whereas treatment with 2 μM ionomycin to increase intracellular calcium caused a translocation of copine-6-GFP to membrane patches (P = 2.6E–7), and the addition of 2 mM EGTA prevented this translocation (Fig. 1*N*,*O*, P = 2.6E–5). Thus, the localization of copine-6-GFP to membranes was calcium-dependent, as previously reported (Perestenko et al. 2010, 2015).

BDNF Upregulates Copine-6 and Recruits it to Synapses

BDNF is essential for long-term potentiation of synaptic strength (Korte et al. 1995), and copine-6 is upregulated by neuronal activity. We therefore tested if BDNF application has any effect on copine-6 expression. Treatment of DIV14 hippocampal slice cultures with 100 ng/ml BDNF for 6 h significantly increased copine-6 expression (P = 0.002), and 48 h treatment increased copine-6 levels further (Fig. 2*A*,*B*, P = 4.1E–4; P = 0.010 for 6 h compared with 48 h BDNF treatment). We then tested if BDNF treatment also alters the subcellular localization of copine-6 in cultured hippocampal neurons. BDNF treatment of DIV14 hippocampal neurons for 48 h recruited copine-6 to synaptic sites marked with synaptophysin (Fig. 2*C*–*E*; P = 1.2E–3 for control compared with 48 h BDNF treatment; P = 0.043 for 6 h compared with 48 h BDNF treatment), and also increased copine-6 in cell somas (Fig. 2*F*; P = 0.020 for control compared with 48 h BDNF treatment). Copine-6 was also significantly increased at synapses by 21 h treatment with 50 μM forskolin (P = 0.011), which induces "LTP-like" enhancement of synaptic strength (Frey et al. 1993), while treatment with 10 μM bicuculline showed a trend toward an increase of copine-6, and 1 μM TTX treatment for 21 h did not change copine-6 levels (Fig. 2*G*; P = 0.031 for comparison between TTX and forskolin treatment).

Copine-6 Alters Dendritic Spine Morphology

Because copine-6 is recruited to dendritic spines by BDNF and LTP-inducing stimuli, we next explored the functional role of copine-6 in relation to spine morphology. Copine-6 was efficiently knocked down by transfection of copine-specific shRNA constructs in hippocampal neurons (Fig. 3*A*). Interestingly, dendritic branching was increased in copine-6 knockdown neurons compared with control neurons transfected with a scrambled shRNA construct (Fig. 3*B*,*C*). To examine dendritic spine morphology in more detail, we cotransfected hippocampal neuron cultures with LifeAct-RFP – to visualize the actin cytoskeleton and monitor any changes in spine morphology – and with EGFP, copine-6-GFP, or copine-6-knockdown constructs. Cultures were additionally immunostained with PSD95 to mark synaptic sites (Fig. 3*D*). Overexpression of copine-6 increased the number of mushroom spines (P = 4.6E–3) and decreased the number of filopodia (P = 2.0E–4). Conversely, knockdown of copine-6 decreased the number of mushroom spines (P = 5.0E–3) and dramatically increased the number of filopodia (Fig. 3*E*; P = 1.0E–5). Knockdown of copine-6 also reduced the number of stubby spines compared with control (P = 1.3E–5). Virtually all mushroom and stubby spines in all conditions had PSD95, while only approximately 20% of filopodia had detectable PSD95 (Fig. 3*E*,*F*; for PSD95-containing mushroom spines P = 3.5E–3 for EGFP/cpne6 and 7.5E–3 for EGFP/cpne6 KD; stubby spines P = 4.1E–5 for EGFP/cpne6 KD; filopodia P = 1.3E–3 for EGFP/cpne6 and 1.1E–5 for EGFP/cpne6 KD). Thus, although knockdown of copine-6 increased the total number of dendritic protrusions (P = 2.0E–4, including filopodia, mushroom and stubby spines) by approximately 30%, this resulted in a concomitant decrease in the overall number of PSD95-positive protrusions (Fig. 3*E*; P = 8.0E–4). The average intensity of PSD95 in PSD95-positive filopodia was also less than that in mushroom or stubby spines (in all conditions). Knockdown or overexpression of copine-6 per se did not change PSD95 intensity, except for a small, but significant, reduction in PSD95 in stubby spines in copine-6 knockdown neurons (Fig. 3*G*; P = 0.024). To confirm the specificity of the copine-6 knockdown, we performed rescue experiments with shRNA-resistant copine-6. We found that the spine phenotype caused by copine-6 knockdown was indeed rescued by co-expression of shRNA-resistant copine-6 (Fig. 4*A*,*B*); mushroom spine number was not significantly different between EGFP and copine-6 rescue neurons (P = 0.480), both of which had less mushroom spines than copine-6 overexpressing neurons (P = 8.7E–5 for EGFP/cpne6 and 2.3E–4 for cpne6 rescue/cpne6) and more mushroom spines than copine-6 knockdown neurons (P = 5.7E–3 for EGFP/cpne6 KD and 9.3E–3 for cpne6 rescue/cpne6 KD). In addition, EGFP and copine-6 rescue neurons had similar numbers of filopodia (P = 0.075) and less filopodia than copine-6 knockdown neurons (P = 1.9E–6 for EGFP/cpne6 KD and 4.8E–6 for cpne6 rescue/cpne6 KD). Together these data show that copine-6 regulates dendritic spine morphology and PSD95 distribution in hippocampal neurons. Loss of copine-6 promotes the formation of new filopodia and increases the relative proportion of filopodia at the expense of mushroom and stubby spines.

Copine-6 Changes mEPSC Kinetics, but not Frequency or Amplitude

Spine morphology is highly correlated with plasticity and efficacy of synaptic connections (Engert and Bonhoeffer 1999; Maletic-Savatic et al. 1999; Kasai et al. 2003). To test if copine-6 affects synaptic transmission, we first recorded mEPSCs from hippocampal neurons transfected with copine-6-GFP, copine-6 knockdown, or EGFP constructs (Fig. 5*A*,*B*). Surprisingly, despite a significant reduction in "mature" dendritic spines harboring PSD95 in copine-6 knockdown neurons (Fig. 3) we found no change in mEPSC amplitude or frequency in copine-6 overexpressing or knockdown neurons, compared with control (Fig. 5*C*,*D*). This suggests that, at least in terms of miniature events, these neurons maintain a normal pool of spontaneously fusing vesicles apposing normal surface levels of AMPA receptors. These

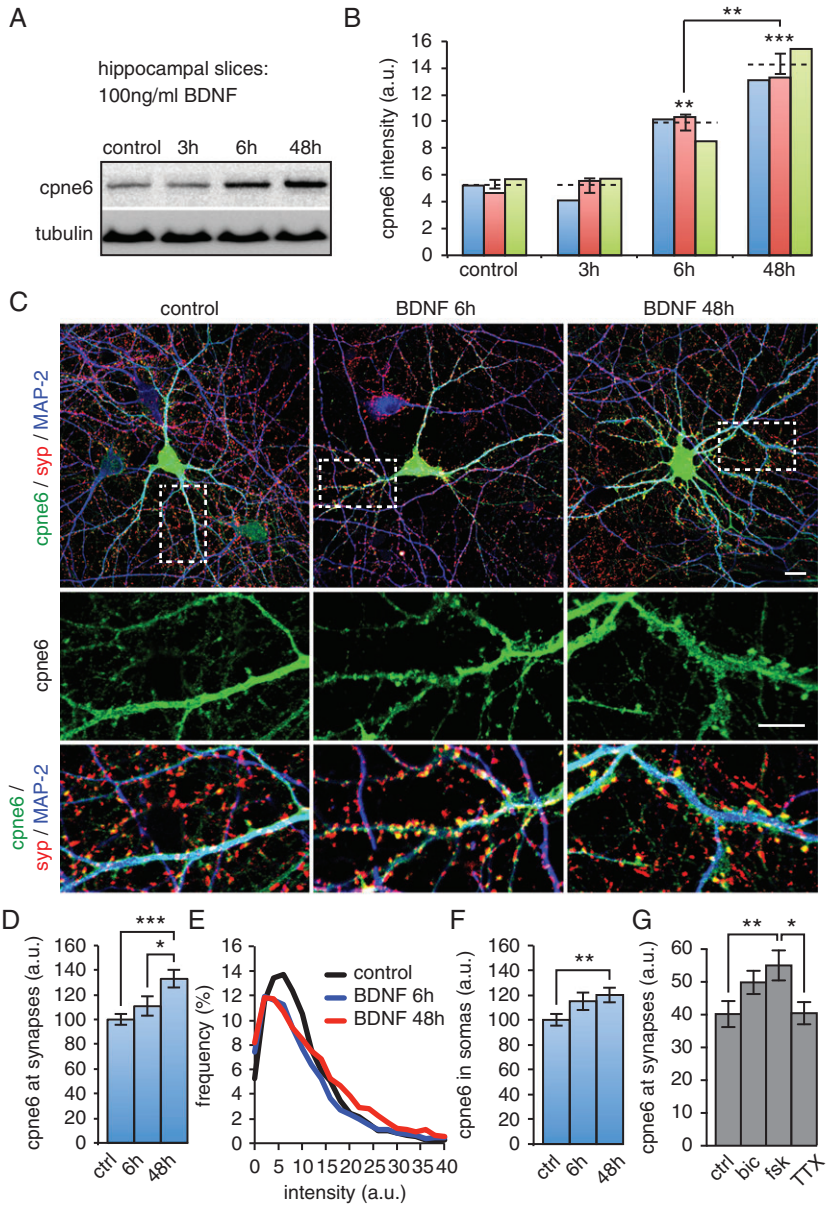

Figure 2. Copine-6 is upregulated and recruited to dendritic spines by BDNF. (*A*) Western blot of control and BDNF-treated cultured hippocampal slices. (*B*) Quantitation of copine-6 signal in Western blots in control conditions and after BDNF treatment in 3 replicates – represented by individual bars; average value is indicated by dashed line – for each condition ($n = 3$, statistical significance determined by two-tailed, type two Student's *t*-test, $P \leq 0.01$ = **, $P \leq 0.001$ = ***). (*C*) Immunostain of DIV14 hippocampal cultures with copine-6, synaptophysin (syp, to mark synapses) and MAP-2 (to mark dendrites) in control conditions and following 100 ng/ml BDNF treatment for 6 h or 48 h. Scale bars = 10 μm in top panels and 5 μm in bottom panels. (*D*) Quantitation of copine-6 intensity at synapses following BDNF treatment in primary hippocampal neurons ($n = 9$ images from 3 different cultures, statistical significance determined by two-tailed, type two Student's *t*-test, $P \leq 0.01$ = **, $P \leq 0.001$ = ***). (*E*) Frequency distribution of copine-6 intensity at synapses (marked with syp) with and without BDNF treatment. (*F*) Intensity of copine-6 in somas in control conditions and following BDNF treatment. Note that non-saturating images with equal gain settings were used for analysis; the images shown in panel C were adjusted for visibility of dendritic spines and thus show saturated cell bodies ($n = 9$ images/3 cultures, statistical significance determined by two-tailed, type two Student's *t*-test, $P \leq 0.01$ = **, $P \leq 0.001$ = ***). (*G*) Quantitation of copine-6 intensity at synapses following treatment with 10 μM bicuculline, 50 μM forskolin, or 1 μM TTX for 21 h, compared with control ($n = 9$ images/3 cultures, statistical significance determined by two-tailed, type two Student's t-test, $P \leq 0.01$ = **, $P \leq 0.001$ = ***).

observations are consistent with reports that ultra-structurally "normal" synapses form on filopodia (Fiala et al. 1998). Interestingly, however, we observed a significant increase in mEPSC rise time ($P = 0.035$) and decay time ($P = 0.043$) in copine-6 knockdown neurons compared with control (Fig. 5*B*,*E*,*F*). This may reflect a change in post-synaptic receptor composition or subunit type in copine-6 knockdown neurons, or represent an "immature" state of synchrony of synaptic vesicle release and post-synaptic receptor composition (Wall et al. 2002). To test the former possibility, we examined surface expression of GluA1, GluA2, and GluN1 receptor subunits in copine-6 overexpressing or knockdown neurons compared with EGFP controls. Transfected neurons were fixed at DIV12, immunostained with antibodies against extracellular epitopes for GluA1, GluA2 or GluN1 in the absence of permeabilization, and the resulting immunofluorescence signal quantified. We found no significant change in intensity (i.e. amount of receptors on the cell surface) for GluA1 (Fig. 5*G*,*H*), GluA2 (Fig. 5*I*,*J*), or GluN1 (Fig. 5*K*,*L*) in copine-6 overexpressing or copine-6

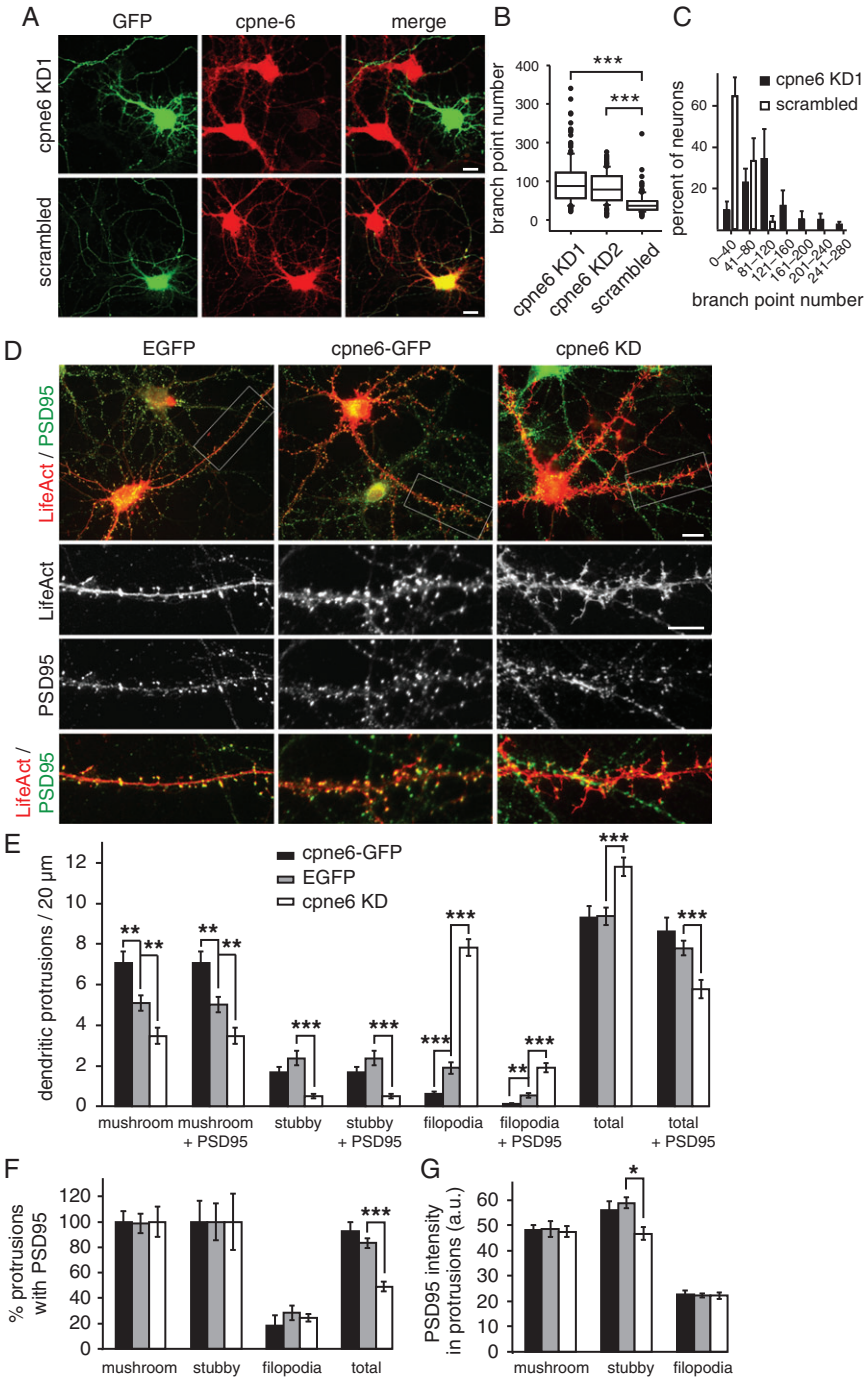

Figure 3. Overexpression and knockdown of copine-6 alters spine number and morphology. (*A*) Images of hippocampal neurons transfected with copine-6 knockdown or scrambled control shRNA constructs at DIV7 and imaged at DIV14. Scale bars are 10 µm. (*B*) Average number of branch points per neuron, in neurons transfected with scrambled shRNA (n = 163) and 2 different copine-6 shRNA constructs inhibiting expression of endogenous copine-6 (n = 170 for copine-6 KD1, n = 106 for copine-6 KD2). For each shRNA, 3 coverslips from each of 3 different cultures were quantified. Statistical significance was determined by a Mann–Whitney U-test. Boxes depict median values, interquartile range and minimum-maximum observations. (*C*) Quantitation of percent of neurons in different bins of 40 branch points each. (*D*) Hippocampal neurons cotransfected with LifeAct-RFP to mark dendritic spines, and EGFP, copine-6-GFP or copine-6 knockdown constructs and immunostained with PSD95 to mark post-synaptic sites. Lower panels show high magnification of the boxes indicated in the upper panels, for each condition. Scale bars = 10 µm in top panels and 5 µm in bottom panels. (*E*) Quantitation of number of filopodia, stubby and mushroom spines, and number of each spine type with PSD95 – in DIV14 EGFP, copine-6-GFP, or copine-6 knockdown transfected neurons. (*F*) Percent of spines of each type in each condition that have PSD95. (*G*) Quantitation of PSD95 intensity in mushroom spines, stubby spines and filopodia (that have detectable PSD95 signal) in transfected neurons (n = 12–14 transfected neurons/2 cultures, statistical significance determined by two-tailed, type two Student's t-test, $P \leq 0.05$ = *, $P \leq 0.01$ = **, $P \leq 0.001$ = ***, for panels E–G).

knockdown neurons compared with EGFP controls, consistent with unchanged mEPSC amplitude (Fig. 5C). Interestingly, the surface expression of GluA1 (the receptor subtype that is inserted into the membrane during LTP) was slightly increased in copine-6 overexpressing neurons compared with EGFP transfected controls, but this increase was not significant (Fig. 5H, P = 0.067).

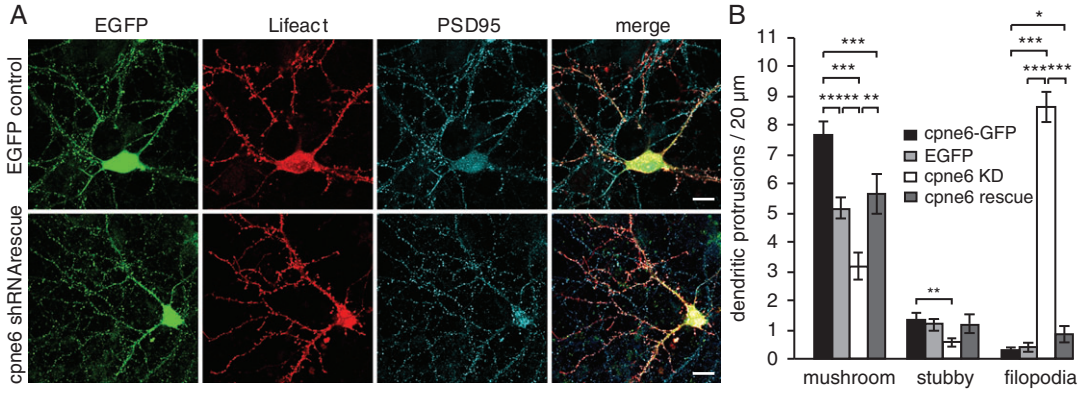

Figure 4. ShRNA-resistant copine-6 rescues the spine phenotype caused by copine-6 knockdown. (*A*) Images of hippocampal neurons cotransfected with LifeAct-RFP to mark dendritic spines, and EGFP or copine-6 knockdown plus shRNA-resistant copine-6, and immunostained with PSD95 to mark post-synaptic sites. Scale bars = 10 µm. (*B*) Quantitation of number of stubby and mushroom spines, and filopodia in EGFP or copine-6 knockdown plus shRNA-resistant copine-6 transfected neurons compared with copine-6-GFP and copine-6 knockdown transfected neurons (n = 8–10 transfected neurons/4 cultures, statistical significance determined by two-tailed, type two Student's t-test, $P \leq 0.05$ = *, $P \leq 0.01$ = **, $P \leq 0.001$ = ***).

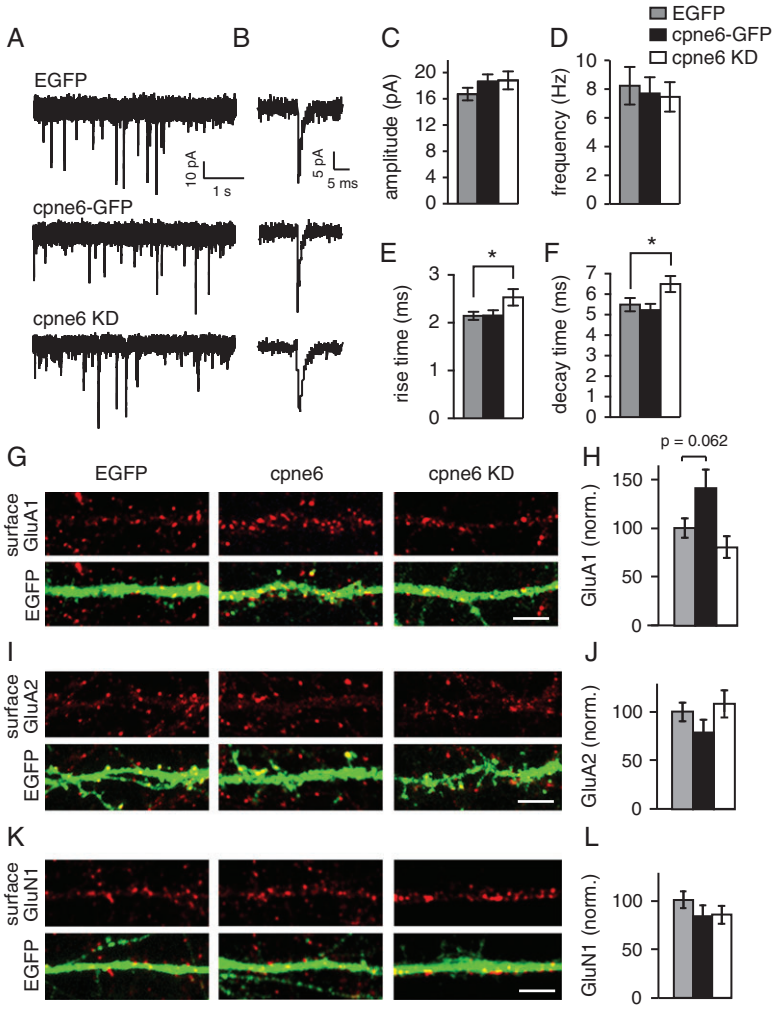

Figure 5. Knockdown of copine-6 increases mEPSC rise and decay time, but does not alter post-synaptic receptor composition. (*A*) Representative mEPSC recordings from EGFP, copine-6-EGFP, and copine-6 knockdown expressing hippocampal neurons. (*B*) High magnification images of representative mEPSCs recorded from DIV14-16 neurons expressing constructs as in panel A, showing increased rise and decay time in copine-6 knockdown neurons. (*C*) Quantitation of mEPSC amplitude, frequency (*D*), rise time (*E*), and decay time (*F*) (n = 18–22 transfected neurons/8 cultures, statistical significance determined by two-tailed, type two Student's t-test, $P \leq 0.05$ = *). (*G*) Immunostains and quantitation (*H*) of intensity of surface GluA1, GluA2 (*I*, *J*) and GluN1 (*K*, *L*) in EGFP, copine-6 overexpressing, and copine-6 knockdown neurons. Scale bars = 5 µm.

Copine-6 Retrogradely Affects Evoked Presynaptic Strength in Contacting Boutons

To examine synaptic vesicle recycling in apposed presynaptic terminals in more detail we performed synaptotagmin (syt)1 antibody uptake assays in depolarizing conditions. Hippocampal neurons were transfected with copine-6 overexpression or knockdown constructs, or EGFP as a control. Our transfection protocol yielded a low efficiency of expression, in only 2–5% of neurons. Thus the majority of presynaptic terminals contacting the dendrites of transfected neurons were wild-type, while the post-synaptic side had increased (overexpressed) or decreased (knocked down) copine-6. Cultures were depolarized by addition of 45 mM KCl in the presence of an antibody against the lumenal domain of syt1 for 10 min. This antibody is taken up by recycling synaptic vesicles, and anti-syt1 signal then serves as a readout of active synapses under evoked conditions, where presynaptic strength can be assessed by intensity of anti-syt1 signal (Fig. 6A). To mark the entire synaptic vesicle pool at synapses, cultures were also labeled with anti-synaptophysin antibody (Fig. 6A).

We found a significant reduction in the total number of presynaptic terminals, identified by synaptophysin, contacting copine-6 knockdown neurons compared with control (Fig. 6B; $P = 8.6E{-}3$), consistent with the reduction in PSD95-positive post-synaptic sites (Fig. 3). The intensity of synaptophysin staining was not altered between conditions, suggesting that the total vesicle pool size at existing synapses is unchanged (Fig. 6C). In addition, the number of synapses with recycling synaptic vesicles, i.e. syt1 uptake, in evoked conditions (Fig. 6D; $P = 0.044$) and the syt1 signal intensity in synaptophysin-positive terminals contacting copine-6 knockdown neurons (Fig. 6E; $P = 9.1E{-}3$) was reduced in copine-6 knockdown neurons compared with control, indicating a decrease in evoked presynaptic strength at existing terminals. Presynaptic terminals innervating copine-6 knockdown neuron filopodia may adopt an "immature" state characterized by high spontaneous release – resulting in normal mEPSC frequency – but lacking the evoked releasable pool of vesicles characteristic of mature, stabilized synaptic sites (Andreae et al. 2012). Alternatively, the relatively modest 20% reduction in presynaptic terminal number in copine-6 knockdown neurons might not be detected as a change in mEPSC frequency given the

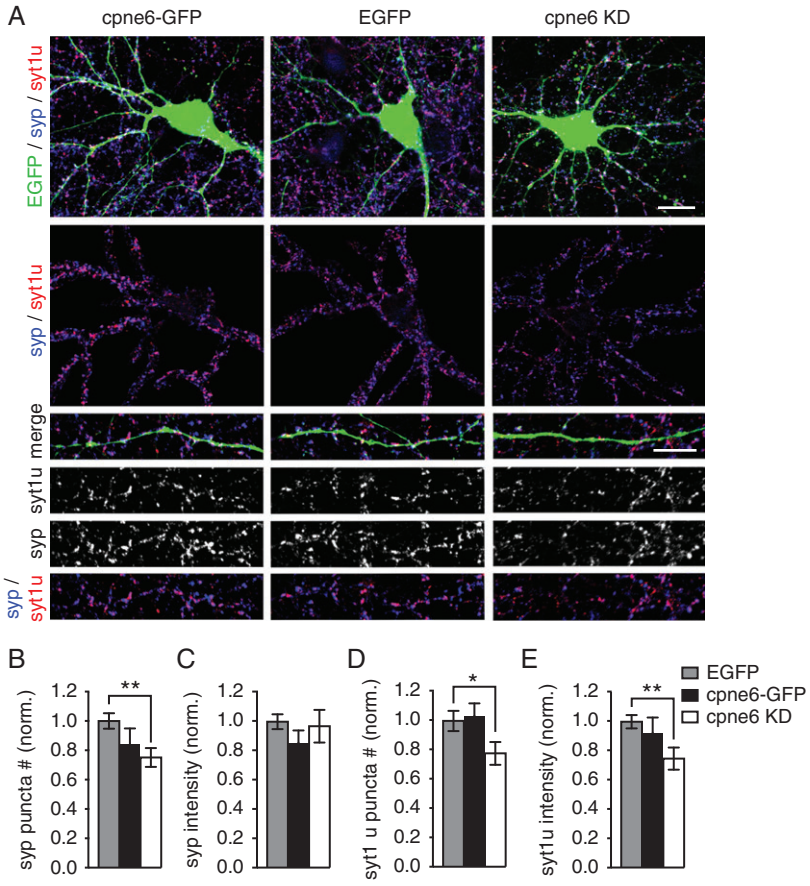

Figure 6. Knockdown of copine-6 changes presynaptic terminal density and evoked synaptic vesicle recycling. (*A*) Immunostains of synaptotagmin (syt)1 luminal antibody uptake in depolarizing conditions (45 mM KCl for 10 min) to mark recycling synaptic vesicles, and synaptophysin to mark total vesicles at presynaptic terminals, in EGFP, copine-6-GFP, and copine-6 knockdown neurons at DIV14. Middle panels show signal for the indicated antibodies in masks of transfected neurons (used for quantitation). Lower panels show representative high magnification images of dendritic regions used to quantify active and total numbers of presynaptic terminals on transfected neurons. Scale bars = 10 μm in top panels and 5 μm in bottom panels. (*B*) Quantitation of synapse number (synaptophysin-positive puncta) on transfected neurons, where loss of copine-6 decreases synapse number. (*C*) Intensity of synaptophysin puncta on neurons transfected with the indicated constructs. (*D*) Quantitation of active synapse number (syt1-positive puncta) on transfected neurons. Loss of copine-6 decreases active synapses. (*E*) Quantitation of syt1 luminal antibody uptake intensity at synaptophysin-positive puncta on neurons transfected with the indicated constructs. Copine-6 knockdown reduces the number of recycling vesicles at synapses ($n = 12$ transfected neurons/4 cultures, statistical significance determined by two-tailed, type two Student's *t*-test, $P \leq 0.05$ = *, $P \leq 0.01$ = ** for panels *H–K*).

variability in mEPSC frequency known to occur in cultured hippocampal neurons. Together these data show that copine-6 not only affects dendritic spine morphology in post-synaptic neurons, but also retrogradely affects evoked presynaptic strength in terminals apposed to dendritic protrusions.

Post-synaptic Knockdown of Copine-6 Decreases LTP and Increases the Early Phase of LTD

Although we found no significant change in mEPSC amplitude or frequency, changes in spine morphology often affect long-term plasticity. We hypothesized that the decrease in mushroom spines and increase in filopodia caused by copine-6 knockdown may affect LTP or LTD. To test this we first validated copine-6 knockdown-EGFP viral injection in the CA1 region of the hippocampus. We found an absence of copine-6 antibody signal coinciding with EGFP signal from copine-6 knockdown in the CA1 region of hippocampal sections (Fig. 7A), verifying successful knockdown. We initially tested input–output relationships of fEPSP magnitude versus stimulation intensity to evaluate post-synaptic responses, and of fEPSP versus fiber volley magnitude to evaluate presynaptic responses (number of axons that give rise to a synaptic response) in EGFP-injected control and copine-6 knockdown injected hippocampal slices. We found no significant change in either parameter (Fig. 7B,C). Thus despite copine-6 knockdown inducing more filopodia and less mushroom spines, basal synaptic transmission is normal. This is consistent with reports that ultra-structurally "normal" synapses form on filopodia (Fiala et al. 1998), and with the unchanged mEPSC frequency and amplitude we observed in copine-6 knockdown neurons (Fig. 5C,D). We also tested paired-pulse facilitation to address potential defects in synaptic vesicle recycling. The paired-pulse ratio was unchanged in copine-6 knockdown injected hippocampal slices compared with EGFP injected controls (Fig. 7D) – suggesting no change in synaptic vesicle recycling in this paradigm. This result is also in agreement with the unchanged mEPSC frequency we observed in copine-6 knockdown neurons.

We then tested LTP and LTD in hippocampal slices in which we knocked down copine-6 post-synaptically by viral injection into the CA1 region, compared with control EGFP virus injected slices. We found that LTP induced by theta burst stimulation was significantly reduced by copine-6 virus injection (Fig. 7E; $P = 0.026$, Mann–Whitney U test). We also found that the initial phase of LTD (up to 25 min after induction) was correspondingly increased in copine-6 knockdown slices compared with control (Fig. 7F; $P = 0.015$; Mann–Whitney U test). These results are consistent with a decrease in "potentiable" mushroom spines and increase in filopodia (lacking PSD-95), in copine-6 knockdown neurons.

Copine-6 is Necessary for BDNF-induced Increases in Mushroom Spine Number

Because copine-6 translocates to spines in response to BDNF treatment, and BDNF increases synaptic strength during long-term potentiation, we reasoned that copine-6 may play a role in

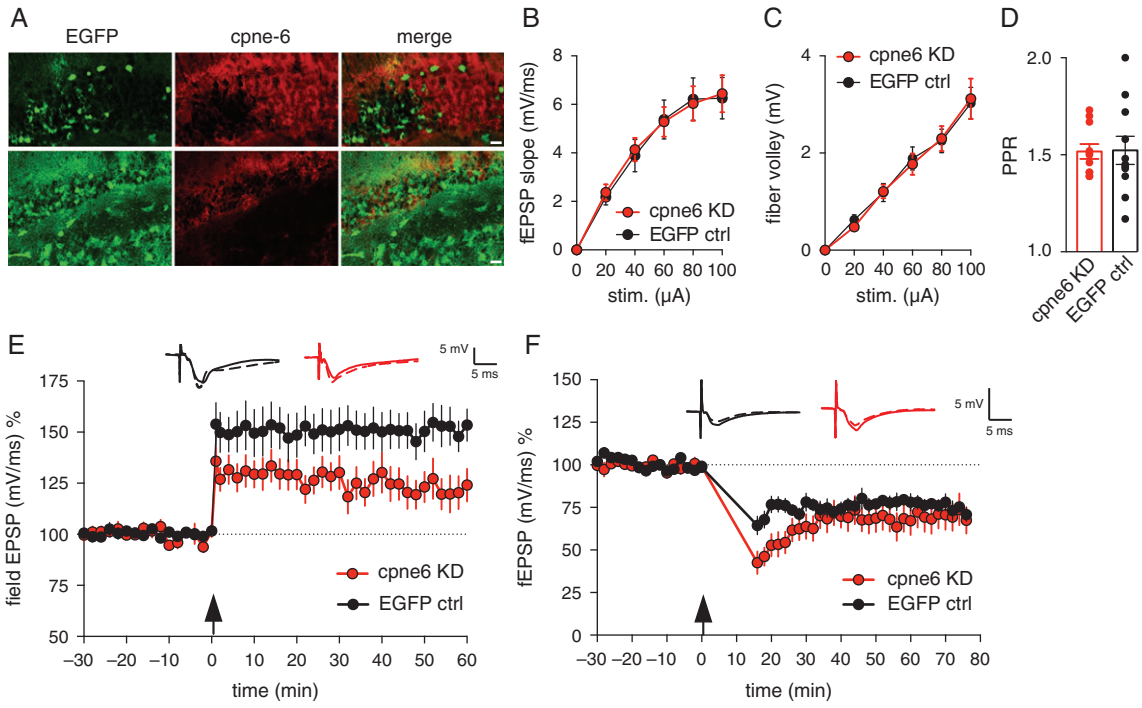

Figure 7. Post-synaptic copine-6 knockdown decreases LTP. (*A*) Representative images from the CA1 region of hippocampal sections of mice injected with copine-6 knockdown AAV virus co-expressing EGFP, immunostained for copine-6. Note that copine-6 signal is reduced in regions with EGFP signal (corresponding to regions where copine-6 is knocked down). Scale bars = 20 μm. (*B*) Input–output relationships of fEPSP magnitude versus stimulation intensity to evaluate post-synaptic responses in hippocampal slices injected with copine-6 knockdown or EGFP control virus ($n = 13$ slices/animals each for cpne6 KD and EGFP injected). (*C*) Input–output relationship of fEPSP versus fiber volley magnitude to evaluate presynaptic responses in EGFP-injected control and copine-6 knockdown injected hippocampal slices ($n = 10$ slices/animals for cpne6 KD and $n = 11$ slices/animals for EGFP). (*D*) Paired-pulse ratio in copine-6 knockdown injected hippocampal slices compared with EGFP injected controls ($n = 11$ slices/animals each for cpne6 KD and EGFP injected). (*E*) LTP in copine-6 knockdown and EGFP control slices. Representative traces indicate fEPSP 30 min before induction (solid line) and 1 h after induction (dashed line); $n = 8$ slices/animals for cpne6 KD and 9 slices for EGFP, $P = 0.026$; significance determined by Mann–Whitney U test. (*F*) LTD in copine-6 knockdown and EGFP control slices. Representative traces indicate fEPSP 30 min before induction (solid line) and 1 h after induction (dashed line); $n = 7$ slices/animals each for cpne6 KD and EGFP, $P = 0.015$; significance determined by Mann–Whitney U test.

BDNF-induced mushroom spine formation. BDNF can promote dendritic spine formation (Ji et al. 2005; Kaneko et al. 2012), and was recently reported to increase the number and spine head width of dendritic spines (Kellner et al. 2014); an effect that may be mediated by copine-6 recruitment to active spines.

To test this we first analyzed dendritic spine morphology following BDNF treatment. We found that 48 h 100 ng/ml BDNF treatment significantly increased the number of mushroom spines compared with control (Fig. 8A,B; $P = 9.9E{-}3$). BDNF treatment of copine-6 knockdown neurons, on the other hand, did not

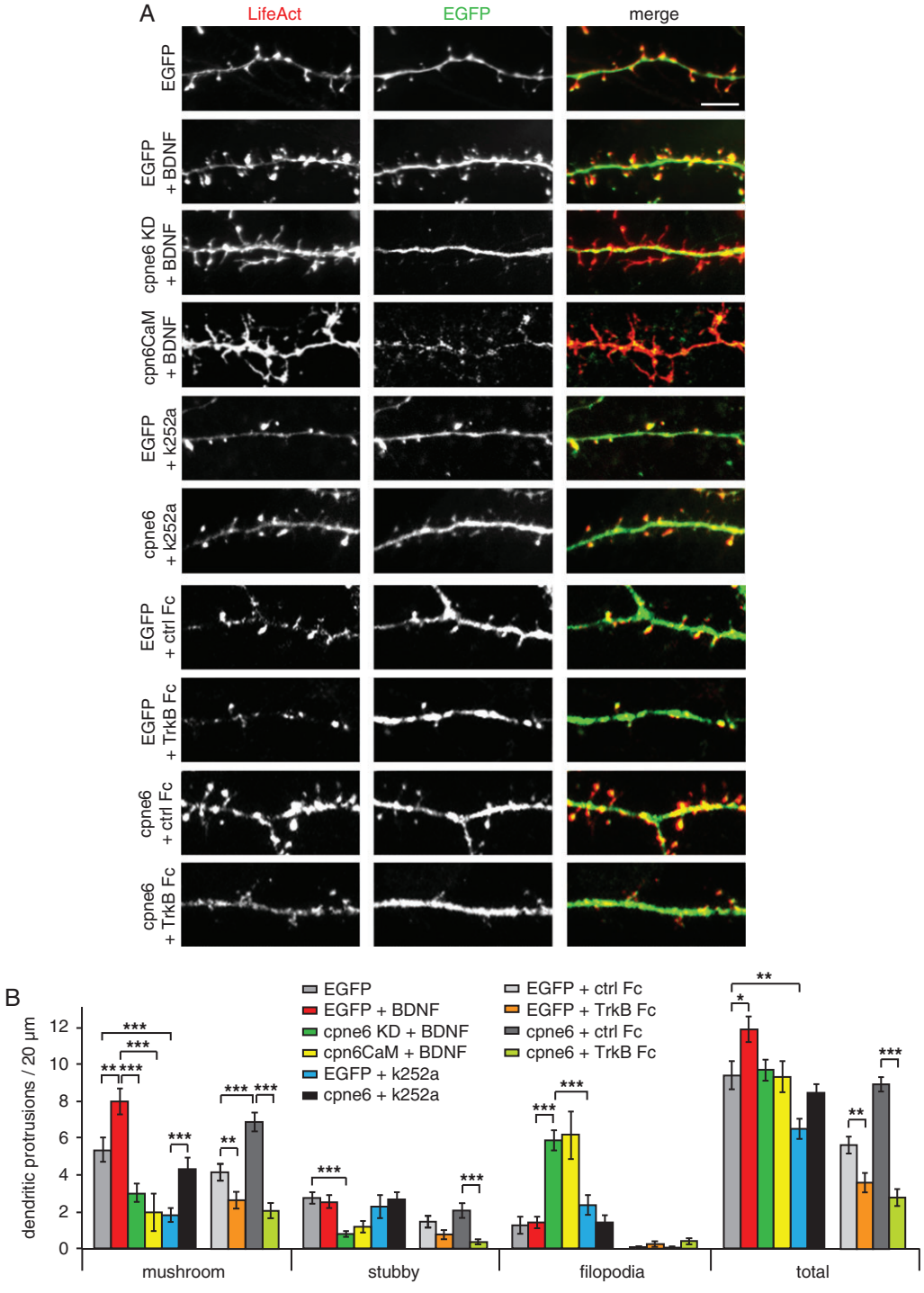

Figure 8. Copine-6 is necessary for BDNF-induced mushroom spine formation. (A) Representative images of dendrites of DIV14 hippocampal neurons cotransfected with LifeAct-RFP to mark dendritic spines, and EGFP, copine-6-GFP, copine-6 knockdown or copine-6 calcium binding mutant (cpne6CaM) constructs with or without 48 h BDNF, k252a, TrkB Fc, or control Fc treatment. Scale bar = 5 µm. (B) Quantitation of number of filopodia, stubby and mushroom spines, and total number of protrusions in each condition (n = 12–14 transfected neurons/3 cultures for each condition, statistical significance determined by two-tailed, type two Student's t-test, $P \leq 0.05$ = *, $P \leq 0.01$ = **, $P \leq 0.001$).

increase mushroom or stubby spine number (P = 2.2E–7 and 9.5E–7, respectively for BDNF-treated EGFP/cpne6 KD), or decrease filopodia number (P = 8.1E–7 for BDNF-treated EGFP/cpne6 KD). BDNF treated knockdown neurons maintained their characteristically high numbers of filopodia, similar to untreated copine-6 knockdown neurons (P = 0.47). There was also no significant difference in mushroom spine number in copine-6 knockdown neurons (Fig. 3) compared with BDNF treated copine-6-knockdown neurons (Fig. 8; P = 0.51), indicating that BDNF and copine-6 are in the same pathway and not in parallel pathways that might each promote mushroom spine formation independently.

Copine-6 binds membranes in a calcium-dependent manner (Perestenko et al. 2010). To test if copine-6 membrane binding is necessary for the BDNF-induced increase in mushroom spines, we transfected neurons with a copine-6 mutant (cpne6CaM), which cannot bind membranes in a calcium-dependent manner (Perestenko et al. 2015). cpne6CaM-expressing neurons treated with BDNF did not show increased mushroom spines (Fig. 8, P = 0.908, P = 4.7E–4 for BDNF-treated EGFP/cpne6CaM) and were identical to copine-6 knockdown neurons in terms of number of mushroom and stubby spines, filopodia, and total number of protrusions (Fig. 8, P = 0.708). Thus calcium-dependent membrane binding of copine-6 is necessary for BDNF-induced increases in mushroom spines.

We further tested the effect of blockade of BDNF signaling on spine morphology by using K252a, a potent inhibitor TrkB receptor tyrosine protein kinase activity (Tapley et al. 1992). Blockade of BDNF signaling significantly reduced the number of mushroom spines and increased the number of filopodia in dendrites (Fig. 8; P = 1.0E–4). Overexpression of copine-6 rescued the number of spines and filopodia in K252a treated neurons to control levels (P = 0.254 and 0.801, respectively, P = 9.6E–4 for K252a treated EGFP/cpne6), indicating that copine-6 acts downstream of BDNF to affect spine morphology.

Because K252a can act as a general kinase inhibitor, we also tested the effect of addition of TrkB Fc, a specific scavenger of BDNF containing the BDNF binding site of the TrkB receptor (Fig. 8). TrkB Fc significantly reduced mushroom (P = 0.019) and stubby (P = 1.1E–5) spine number compared with control Fc treated cultures. Copine-6 overexpressed cells treated with control Fc had significantly more mushroom spines than EGFP controls treated with Fc (P = 1.7E–4), and addition of TrkB Fc reduced mushroom spine number in copine-6 overexpressing neurons (P = 6.4E–7), to levels similar to EGFP controls treated with TrkB Fc (P = 0.356). This further confirms that copine-6 affects spine morphology downstream of BDNF (Fig. 8; for total spines P = 0.021 for EGFP/EGFP + BDNF, P = 6.6E–3 for EGFP/EGFP + K252a, P = 4.4E–3 for EGFP + ctrl Fc/EGFP + TrkB Fc, and P = 2.4E–7 for cpne6 + ctrl Fc/cpne6 + TrkB Fc).

Copine-6 Interacts with TrkB and Facilitates its Recycling to the Cell Surface

Because copine-6 is recruited to plasma membranes and necessary for BDNF-dependent changes in spine morphology, we tested if copine-6 might interact with the TrkB receptor. We co-expressed HA-TrkB and copine-6-GFP in HEK cells, and performed co-immunoprecipitation using an HA antibody conjugated to beads. We found that copine-6 and TrkB did indeed interact in this assay. HA antibody conjugated beads pulled down HA-TrkB from HEK cell lysates (Fig. 9A) and also pulled down copine-6-GFP (Fig. 9B).

We next tested if copine-6 levels might affect the surface expression or recycling of TrkB. We co-expressed copine-6, copine-6 knockdown or EGFP with HA-TrkB in hippocampal neurons by transfection on DIV10, where the extracellular HA epitope enabled us (on DIV13) to label both surface HA-TrkB (in non-permeabilizing conditions) and total internal HA-TrkB following permeabilization. We then quantified the relative surface to internal HA-TrkB signal in each condition. EGFP and copine-6 knockdown neurons showed similar levels of surface HA-TrkB in control conditions, and similarly significant internalization of HA-TrkB following 15 min of 100 ng/ml BDNF treatment (Fig. 9C–E; P = 1.5E–3 for EGFP control compared with BDNF-treated, P = 0.027 for copine-6 KD control compared with BDNF-treated). However, overexpression of copine-6 increased surface expression of HA-TrkB in control conditions (Fig. 9C,F; P = 0.031), and surface expression remained significantly higher in copine-6 overexpressing neurons compared with EGFP expressing controls, even following BDNF treatment (Fig. 9D,E; P = 6.0E–4). This could result from a decrease in BDNF-dependent TrkB endocytosis, or an increase in the recycling of TrkB back to the surface in copine-6 overexpressing neurons following BDNF treatment. To distinguish between these 2 possibilities, we performed an additional assay in which DIV13 neurons co-expressing HA-TrkB and EGFP, copine-6 or copine-6 knockdown were labeled live with HA antibody. Cells were then treated with BDNF for 30 min (during which activated TrkB receptors are expected to be internalized). The remaining surface HA antibody was then stripped by treatment with 0.04% EDTA, and cells were allowed to recover for 40 min, during which some proportion of internalized TrkB is recycled back to the surface (Huang et al. 2013). Cells were then stained with a secondary antibody against HA to mark HA-TrkB that was recycled back to the surface following internalization. We quantified recovery of surface HA-TrkB by normalizing HA-TrkB recycled back to the surface to control surface levels without BDNF stimulation for each condition (EGFP, copine-6 overexpressing, or copine-6 knockdown). This revealed that EGFP control neurons recovered approximately 19% of HA-TrkB surface fluorescence in the 40 min following BDNF treatment. Copine-6 overexpressing neurons recovered 32% – significantly more than control (P = 0.040). And copine-6 knockdown neurons recovered 10% – only half as much as control (P = 0.007) (Fig. 9F,G; P = 5.0E–4 for copine-6 overexpressed compared with copine-6 knockdown). These data indicate that copine-6 promotes surface expression of TrkB receptors.

We hypothesized that alterations in surface expression of TrkB would subsequently affect downstream BDNF-TrkB signaling. To test this, we examined the levels of phospho-ERK, which signals downstream of BDNF-TrkB and and is necessary for BDNF-TrkB-dependent increases in mushroom spines (Alonso et al. 2004). Phospho-ERK would be expected to increase following more activation of TrkB, and decrease following less activation of TrkB. We found that overexpression of copine-6 indeed increased p-ERK levels (Fig. 9H,I; P = 0.0286), consistent with an increase in BDNF-TrkB signaling induced by copine-6. Conversely, knockdown of copine-6 decreased p-ERK levels compared with control neurons (Fig. 9H,I; P = 0.0132). These results are consistent with copine-6 promoting increased surface expression of TrkB and subsequent downstream signaling to affect spine morphology.

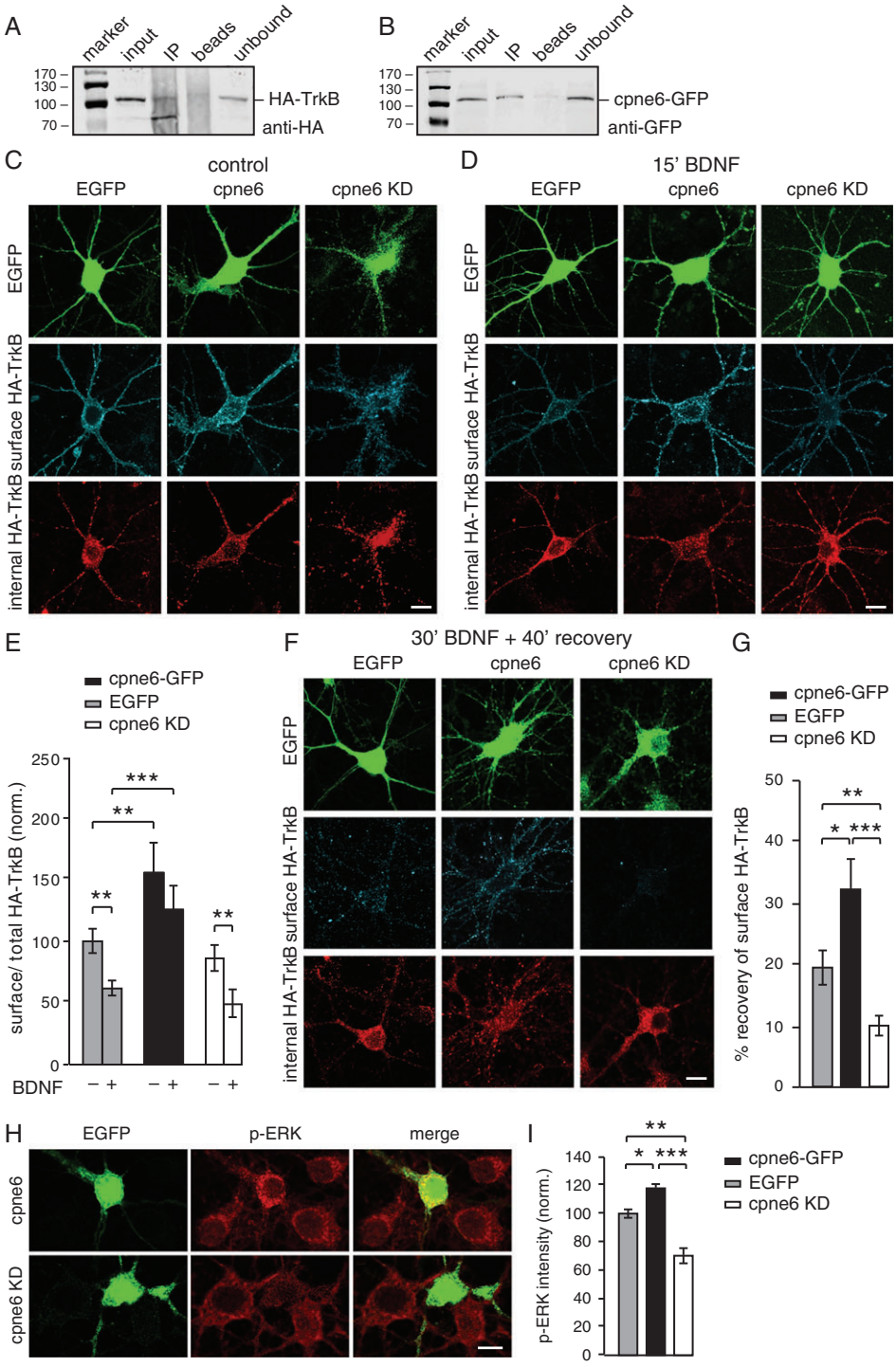

Figure 9. Copine-6 promotes surface expression of the TrkB receptor. (*A*) Western blot of immunoprecipitation, using an HA antibody, of HA-TrkB and cpne6-GFP (*B*) co-expressed in HEK cells and blotted for HA or GFP, respectively. (*C*) Images of hippocampal neurons cotransfected with HA-TrkB and EGFP, copine-6, or copine-6 knockdown and immunostained for surface and internal HA-TrkB in control conditions, and following 100 ng/ml BDNF treatment for 30 min (*D*). *E*) Quantitation of surface/total HA-TrkB in control (*C*) and BDNF-treated (*D*) conditions, normalized to control EGFP (n = 22–59 transfected neurons/3 cultures for each condition, statistical significance determined by two-tailed, type two Student's t-test, $P \leq 0.01$ = **, $P \leq 0.001$). (*F*) Images of neurons cotransfected with HA-TrkB and EGFP, copine-6 or copine-6 knockdown after live labeling with HA antibody, BDNF treatment for 30 min (during which activated TrkB receptors are internalized), stripping of remaining HA antibody from the surface, allowing cells to recover for 40 min (during which TrkB is recycled back to the surface), and labeling with a secondary antibody against HA to mark HA-TrkB that recycled back to the surface compared with total internal HA-TrkB labeled after permeabilization. (*G*) Quantitation of % recovery of surface TrkB (*E*) normalized to control (*C*) for each condition (n = 23–27 transfected neurons/3 cultures for each condition, statistical significance determined by two-tailed, type two Student's t-test, $P \leq 0.05$ = *, $P \leq 0.01$ = **, $P \leq 0.001$). (*H*) Immunostains of copine-6 overexpressing and copine-6 knockdown neurons for phospho-ERK. (*I*) Quantitation of P-ERK antibody fluorescence intensity in copine-6 overexpressing and copine-6 knockdown neurons, normalized to control untransfected cells.

Discussion

In summary we identified a novel function of copine-6, in regulating dendritic spine morphology. Copine-6 knockdown reduces the number of mushroom spines and dramatically increases the number of filopodia, which lack PSD95; Copine-6 overexpression increases the number of mushroom spines. In addition, presynaptic strength in terminals contacting copine-6 knockdown neurons is decreased. Knockdown of copine-6 post-synaptically in the CA1 region of the hippocampus decreased Schaffer collateral LTP and increased the initial phase of LTD. Mechanistically, we found that copine-6 binds TrkB, and promotes its surface expression and recycling back to the plasma membrane following activation, thus promoting BDNF-TrkB signaling and increasing the number of mushroom spines in hippocampal dendrites.

We found that copine-6 protein expression begins postnatally, and increases with activity, consistent with earlier reports (Nakayama et al. 1998). Copine-6 may therefore act during synaptic plasticity to strengthen and stabilize potentiated synapses – a feature that is necessary for adjustments in synapse strength based on experience, most notably during learning and memory. BDNF is widely regarded as playing a key role in this process (Bramham and Messaoudi 2005). Indeed, we found that BDNF increases mushroom spine number, and this effect depends on copine-6.

Copine-6 can sense calcium via its C2-domains and translocate to cell membranes in a calcium-dependent manner (Creutz et al. 1998; Damer et al. 2005; Perestenko et al. 2010). The compartmentalization of calcium in dendritic spines (Muller and Connor 1991) would potentially allow tight control of dendritic spine morphology at individual synaptic sites by copine-6. Highly active synapses with greater calcium influx might recruit copine-6 (and therefore more plasma membrane-localized TrkB) and become stabilized, while inactive synapses might have less calcium influx, less copine-6 and surface expression of TrkB, become destabilized and revert to a filopodial state and perhaps eventually be eliminated. Upregulation of copine-6 by neuronal activity would increase the levels of copine-6 in active neurons, while changes in calcium in individual spines would concomitantly increase the proportion of membrane-bound copine-6 to alter the morphology of individual spines. The calcium-dependent translocation of cytosolic copine-6 to membranes might act to initiate BDNF-TrkB signaling to translate changes in neuronal activity into morphological changes in dendritic spine membranes.

Copine-6 is similar in many respects to calcium/calmodulin-dependent protein kinase II (CaMKII). CaMKII is recruited specifically into active spines (Shen and Meyer 1999), and requires activation by calcium influx via the NMDA receptor (Lee et al. 2009). CaMKII is important for long-term potentiation of synaptic strength and stabilizes synapses via interaction with several other proteins (Hell 2014). Although copines do not harbor any signaling domains themselves, we found that copine-6 binds the TrkB receptor and promotes its delivery to the cell surface, thus enhancing BDNF-TrkB signaling cascades (including activation of ERK). Copines interact with a number of other proteins involved in intracellular signaling pathways, including MEK1, protein phosphatase 5, and Cdc42-regulated kinase (Tomsig et al. 2003). Copine-6 may, like CamKII, be integral to initiation of signaling cascades important for dendritic spine morphology and synaptic function.

A recent study also reported copine-6 involvement in dendritic spine remodeling (Reinhard et al. 2016). We observed recruitment of endogenous copine-6 to spines by BDNF using our antibody, in agreement with translocation of overexpressed copine-6-GFP to the plasma membrane by NMDA receptor activation observed by Reinhard et al. However, we detected copine-6 expression in brain by E18, while Reinhard et al. reported later onset at P7. In addition, we found that copine-6 knockdown and expression of a copine-6 calcium mutant both dramatically increased filopodia and decreased mushroom spines, and copine-6 overexpression did the opposite. But Reinhard et al. found that neither copine-6 knockout, expression of a copine-6 calcium binding mutant, nor copine-6 overexpression altered spine density or morphology. Rather, knockout of copine-6 prevented a chemical-LTP induced increase in spine head width (Reinhard et al. 2016). Consistent with the dramatic decrease in mushroom spines we observed in copine-6 knockdown neurons, we found a decrease in LTP and increase in early phase LTD in hippocampal slices in which copine-6 was knocked down post-synaptically. Reinhard et al., on the other hand, found normal induction of LTP in copine-6 constitutive knockouts, but a faster decay (reduced maintenance) of LTP, and no change in LTD. These differences in findings could be due to compensation for lack of copine-6 in the knockout mice used in Reinhard et al., while the copine-6 knockdown approach we employed is more acute and might not allow for a compensatory mechanism.

Mechanistically, Reinhard et al. propose that copine-6 acts in the Rac1-PAK-LIMK1-Cofilin pathway to regulate structural plasticity of dendritic spines, based on observations that there is less GFP-Rac1 in spines of neurons cotransfected with calcium mutant copine-6 and that copine-6 and Rac1 co-IP from transfected cells (Reinhard et al. 2016). We propose that copine-6 regulates BDNF-TrkB signaling, based on our finding that copine-6 promotes recycling of activated TrkB to the plasma membrane, and increases BDNF-TrkB signaling to affect spine morphology, and that copine-6 and TrkB co-IP. Nonetheless, there is agreement that copine-6 is important for aspects of dendritic spine morphology and plasticity.

Alterations in spine stability and morphology occur not only during development and adult plasticity in the normal brain, but also in neurodegenerative and neurodevelopmental diseases, including autism and Fragile X syndrome (van Spronsen and Hoogenraad 2010). The increase in filopodia and loss of mushroom spines in copine-6 knockdown neurons is reminiscent of Fragile X syndrome, in which filopodia and overall spine numbers are increased and synaptic contact area on spines is reduced (Irwin et al. 2000). Our study opens an avenue into investigation of these aspects of copine-6 function and its regulation of BDNF-TrkB signaling in plasticity as well as brain disorders such as autism and Fragile X syndrome.

Supplementary Material

Supplementary material is available at *Cerebral Cortex* online.

Funding

Dorothea Schloezer fellowship to K.B., a Sofja Kovalevskaja grant from the Alexander von Humboldt Foundation, European Research Council starting grant SytActivity FP7 260916, Deutsche Forschungsgemeinschaft grants CRC889, DE1951/1-1 and Center for Nanoscale Microscopy and Molecular Physiology of the Brain (CNMPB) to C.D., and by the Medical Research Council UK to J.M. and P.P.

Notes

We thank Thomas Dresbach for critique of the manuscript. *Conflict of Interest*: The authors declare that they have no conflict of interest. Author contributions are KB: Fig. 1CFO, 4, 5G-L, 7A, 8, 9, Suppl. Fig. 1B; BR: Fig. 1DEHI, 2AB, 7B-F; SA: Fig. 1ACDEJKLM, 2AB; JHZ: Fig. 1GI, 2-G, 6; AA: Fig. 1N, 3D-G, 5A-F; EB: Fig. 7, Suppl. Fig. 1B; RF: Fig. 1B; PP: Fig. 3A-C, Suppl. Fig. 1A; CD: Fig. 3D-G, 4B. Experimental Assistance: HA, AS; Conceptualization and Funding Acquisition: JM, AS, PP, CD; Writing: SA, CD.

References

Ahmed S, Wittenmayer N, Kremer T, Hoeber J, Kiran Akula A, Urlaub H, Islinger M, Kirsch J, Dean C, Dresbach T. 2013. Mover is a homomeric phospho-protein present on synaptic vesicles. PloS One. 8:e63474.

Alonso M, Medina JH, Pozzo-Miller L. 2004. ERK1/2 activation is necessary for BDNF to increase dendritic spine density in hippocampal CA1 pyramidal neurons. Learn Mem. 11:172–178.

Andreae LC, Fredj NB, Burrone J. 2012. Independent vesicle pools underlie different modes of release during neuronal development. J Neurosci. 32:1867–1874.

Araya R, Jiang J, Eisenthal KB, Yuste R. 2006. The spine neck filters membrane potentials. Proc Natl Acad Sci USA. 103: 17961–17966.

Banker G, Goslin K. 1988. Developments in neuronal cell culture. Nature. 336:185–186.

Bliss TV, Collingridge GL. 1993. A synaptic model of memory: long-term potentiation in the hippocampus. Nature. 361: 31–39.

Bosch M, Castro J, Saneyoshi T, Matsuno H, Sur M, Hayashi Y. 2014. Structural and molecular remodeling of dendritic spine substructures during long-term potentiation. Neuron. 82:444–459.

Boyken J, Gronborg M, Riedel D, Urlaub H, Jahn R, Chua JJ. 2013. Molecular profiling of synaptic vesicle docking sites reveals novel proteins but few differences between glutamatergic and GABAergic synapses. Neuron. 78:285–297.

Bramham CR, Messaoudi E. 2005. BDNF function in adult synaptic plasticity: the synaptic consolidation hypothesis. Prog Neurobiol. 76:99–125.

Choy RW, Park M, Temkin P, Herring BE, Marley A, Nicoll RA, von Zastrow M. 2014. Retromer mediates a discrete route of local membrane delivery to dendrites. Neuron. 82:55–62.

Comery TA, Harris JB, Willems PJ, Oostra BA, Irwin SA, Weiler IJ, Greenough WT. 1997. Abnormal dendritic spines in fragile X knockout mice: maturation and pruning deficits. Proc Natl Acad Sci USA. 94:5401–5404.

Creutz CE, Tomsig JL, Snyder SL, Gautier MC, Skouri F, Beisson J, Cohen J. 1998. The copines, a novel class of C2 domain-containing, calcium-dependent, phospholipid-binding proteins conserved from Paramecium to humans. J Biol Chem. 273:1393–1402.

Damer CK, Bayeva M, Hahn ES, Rivera J, Socec CI. 2005. Copine A, a calcium-dependent membrane-binding protein, transiently localizes to the plasma membrane and intracellular vacuoles in Dictyostelium. BMC Cell Biol. 6:46.

Engert F, Bonhoeffer T. 1999. Dendritic spine changes associated with hippocampal long-term synaptic plasticity. Nature. 399:66–70.

Fiala JC, Feinberg M, Popov V, Harris KM. 1998. Synaptogenesis via dendritic filopodia in developing hippocampal area CA1. J Neurosci. 18:8900–8911.

Frey U, Huang YY, Kandel ER. 1993. Effects of cAMP simulate a late stage of LTP in hippocampal CA1 neurons. Science. 260: 1661–1664.

Fuller L, Dailey ME. 2007. Preparation of rodent hippocampal slice cultures. CSH Protocols. 2007:pdb prot4848.

Harnett MT, Makara JK, Spruston N, Kath WL, Magee JC. 2012. Synaptic amplification by dendritic spines enhances input cooperativity. Nature. 491:599–602.

Harris KM, Jensen FE, Tsao B. 1992. Three-dimensional structure of dendritic spines and synapses in rat hippocampus (CA1) at postnatal day 15 and adult ages: implications for the maturation of synaptic physiology and long-term potentiation. J Neurosci. 12:2685–2705.

Hell JW. 2014. CaMKII: claiming center stage in postsynaptic function and organization. Neuron. 81:249–265.

Hotulainen P, Hoogenraad CC. 2010. Actin in dendritic spines: connecting dynamics to function. J Cell Biol. 189: 619–629.

Huang SH, Wang J, Sui WH, Chen B, Zhang XY, Yan J, Geng Z, Chen ZY. 2013. BDNF-dependent recycling facilitates TrkB translocation to postsynaptic density during LTP via a Rab11-dependent pathway. J Neurosci. 33:9214–9230.

Huttner WB, Schiebler W, Greengard P, De Camilli P. 1983. Synapsin I (protein I), a nerve terminal-specific phosphoprotein. III. Its association with synaptic vesicles studied in a highly purified synaptic vesicle preparation. J Cell Biol. 96:1374–1388.

Irwin SA, Galvez R, Greenough WT. 2000. Dendritic spine structural anomalies in fragile-X mental retardation syndrome. Cereb Cortex. 10:1038–1044.

Ji Y, Pang PT, Feng L, Lu B. 2005. Cyclic AMP controls BDNF-induced TrkB phosphorylation and dendritic spine formation in mature hippocampal neurons. Nat Neurosci. 8: 164–172.

Kaneko M, Xie Y, An JJ, Stryker MP, Xu B. 2012. Dendritic BDNF synthesis is required for late-phase spine maturation and recovery of cortical responses following sensory deprivation. J Neurosci. 32:4790–4802.

Kasai H, Matsuzaki M, Noguchi J, Yasumatsu N, Nakahara H. 2003. Structure-stability-function relationships of dendritic spines. Trends Neurosci. 26:360–368.

Kellner Y, Godecke N, Dierkes T, Thieme N, Zagrebelsky M, Korte M. 2014. The BDNF effects on dendritic spines of mature hippocampal neurons depend on neuronal activity. Front Synaptic Neurosci. 6:5.

Korte M, Carroll P, Wolf E, Brem G, Thoenen H, Bonhoeffer T. 1995. Hippocampal long-term potentiation is impaired in mice lacking brain-derived neurotrophic factor. Proc Natl Acad Sci USA. 92:8856–8860.

Lee SJ, Escobedo-Lozoya Y, Szatmari EM, Yasuda R. 2009. Activation of CaMKII in single dendritic spines during long-term potentiation. Nature. 458:299–304.

Maletic-Savatic M, Malinow R, Svoboda K. 1999. Rapid dendritic morphogenesis in CA1 hippocampal dendrites induced by synaptic activity. Science. 283:1923–1927.

Matsuzaki M, Ellis-Davies GC, Nemoto T, Miyashita Y, Iino M, Kasai H. 2001. Dendritic spine geometry is critical for AMPA receptor expression in hippocampal CA1 pyramidal neurons. Nat Neurosci. 4:1086–1092.

Matsuzaki M, Honkura N, Ellis-Davies GC, Kasai H. 2004. Structural basis of long-term potentiation in single dendritic spines. Nature. 429:761–766.

Muller W, Connor JA. 1991. Dendritic spines as individual neuronal compartments for synaptic Ca2+ responses. Nature. 354:73–76.

Nagerl UV, Eberhorn N, Cambridge SB, Bonhoeffer T. 2004. Bidirectional activity-dependent morphological plasticity in hippocampal neurons. Neuron. 44:759–767.

Nakayama AY, Harms MB, Luo L. 2000. Small GTPases Rac and Rho in the maintenance of dendritic spines and branches in hippocampal pyramidal neurons. J Neurosci. 20:5329–5338.

Nakayama T, Yaoi T, Kuwajima G. 1999. Localization and subcellular distribution of N-copine in mouse brain. J Neurochem. 72:373–379.

Nakayama T, Yaoi T, Yasui M, Kuwajima G. 1998. N-copine: a novel two C2-domain-containing protein with neuronal activity-regulated expression. FEBS Lett. 428:80–84.

Newpher TM, Ehlers MD. 2009. Spine microdomains for postsynaptic signaling and plasticity. Trends Cell Biol. 19: 218–227.

Nimchinsky EA, Sabatini BL, Svoboda K. 2002. Structure and function of dendritic spines. Annu Rev Physiol. 64:313–353.

Pandey K, Sharma SK. 2011. Activity-dependent acetylation of alpha tubulin in the hippocampus. In: J Mol Neurosci. 45:1–4.

Penzes P, Cahill ME, Jones KA, VanLeeuwen JE, Woolfrey KM. 2011. Dendritic spine pathology in neuropsychiatric disorders. Nat Neurosci. 14:285–293.

Perestenko P, Watanabe M, Beusnard-Bee T, Guna P, McIlhinney J. 2015. The second C2-domain of copine-2, copine-6 and copine-7 is responsible for their calcium-dependent membrane association. FEBS J. 282:3722–3736.

Perestenko PV, Pooler AM, Noorbakhshnia M, Gray A, Bauccio C, Jeffrey McIlhinney RA. 2010. Copines-1, -2, -3, -6 and -7 show different calcium-dependent intracellular membrane translocation and targeting. FEBS J. 277:5174–5189.

Ramachandran B, Frey JU. 2009. Interfering with the actin network and its effect on long-term potentiation and synaptic tagging in hippocampal CA1 neurons in slices in vitro. J Neurosci. 29:12167–12173.

Ramachandran B, Ahmed S, Zafar N, Dean C. 2015. Ethanol inhibits long-term potentiation in hippocampal CA1 neurons, irrespective of lamina and stimulus strength, through neurosteroidogenesis. Hippocampus. 25:106–118.

Reinhard JR, Kriz A, Galic M, Angliker N, Rajalu M, Vogt KE, Ruegg MA. 2016. The calcium sensor Copine-6 regulates spine structural plasticity and learning and memory. Nat Commun. 7:11613.

Sala C, Segal M. 2014. Dendritic spines: the locus of structural and functional plasticity. Physiol Rev. 94:141–188.

Shen K, Meyer T. 1999. Dynamic control of CaMKII translocation and localization in hippocampal neurons by NMDA receptor stimulation. Science. 284:162–166.

Svoboda K, Tank DW, Denk W. 1996. Direct measurement of coupling between dendritic spines and shafts. Science. 272:716–719.

Tang G, Gudsnuk K, Kuo SH, Cotrina ML, Rosoklija G, Sosunov A, Sonders MS, Kanter E, Castagna C, Yamamoto A, et al. 2014. Loss of mTOR-dependent macroautophagy causes autistic-like synaptic pruning deficits. Neuron. 83:1131–1143.

Tapley P, Lamballe F, Barbacid M. 1992. K252a is a selective inhibitor of the tyrosine protein kinase activity of the trk family of oncogenes and neurotrophin receptors. Oncogene. 7:371–381.

Tomsig JL, Snyder SL, Creutz CE. 2003. Identification of targets for calcium signaling through the copine family of proteins. Characterization of a coiled-coil copine-binding motif. J Biol Chem. 278:10048–10054.

Tonnesen J, Katona G, Rozsa B, Nagerl UV. 2014. Spine neck plasticity regulates compartmentalization of synapses. Nat Neurosci. 17:678–685.

van Spronsen M, Hoogenraad CC. 2010. Synapse pathology in psychiatric and neurologic disease. Curr Neurol Neurosci Rep. 10:207–214.

Wall MJ, Robert A, Howe JR, Usowicz MM. 2002. The speeding of EPSC kinetics during maturation of a central synapse. Eur J Neurosci. 15:785–797.

Xu T, Yu X, Perlik AJ, Tobin WF, Zweig JA, Tennant K, Jones T, Zuo Y. 2009. Rapid formation and selective stabilization of synapses for enduring motor memories. Nature. 462:915–919.

Yang G, Pan F, Gan WB. 2009. Stably maintained dendritic spines are associated with lifelong memories. Nature. 462: 920–924.

Yoshihara Y, De Roo M, Muller D. 2009. Dendritic spine formation and stabilization. Curr Opin Neurobiol. 19:146–153.

Zhou Q, Homma KJ, Poo MM. 2004. Shrinkage of dendritic spines associated with long-term depression of hippocampal synapses. Neuron. 44:749–757.